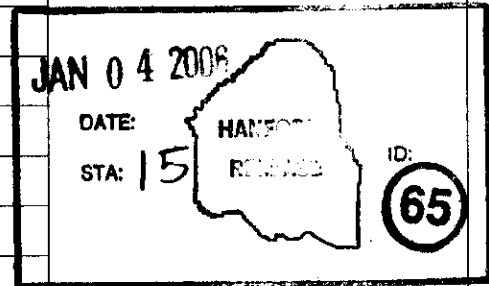


## CH2M HILL DOCUMENT RELEASE FORM

(1) Document Number: RPP-13310		(2) Revision Number: 1	(3) Effective Date: on release
(4) Document Type: <input type="checkbox"/> Digital Image <input type="checkbox"/> Hard copy <input checked="" type="checkbox"/> PDF <input type="checkbox"/> Video		(a) Number of pages (including the DRF) or number of digital images: 79	
(5) Release Type <input type="checkbox"/> New <input type="checkbox"/> Cancel		<input type="checkbox"/> Page Change <input checked="" type="checkbox"/> Complete Revision	
(6) Document Title: Modeling Data Package for an Initial Assessment of Closure of the C Tank Farm			
(7) Change/Release Description: Complete revision			
(8) Change Justification: NA			
(9) Associated Structure, System, and Component (SSC) and Building Number:	(a) Structure Location: NA		(c) Building Number: NA
	(b) System Designator: NA		(d) Equipment ID Number (EIN): NA
(10) Impacted Documents:	(a) Document Type	(b) Document Number	(c) Document Revision
	NA		
(11) Approvals:			
(a) Author (Print/Sign): M.P. Connelly <i>M.P. Connelly</i>		Date: 01/03/06	
(b) Responsible Manager (Print/Sign): F.J. Anderson <i>Frank Anderson</i>		Date: 01/03/06	
(c) Reviewer (Optional, Print/Sign):		Date:	
(d) Reviewer (Optional, Print/Sign):		Date:	
(12) Distribution:			
(a) Name	(b) MSIN	(a) Name	(b) MSIN
R. Khaleel	E6-17		
M.P. Connelly	H6-03		
W.J. McMahon	H6-03		
M.I. Wood	H8-44		
F.J. Anderson (3H)	H6-03		
DOE/RL Reading Room (H)	H2-53		
(13) Clearance		(a) Cleared for Public Release <input checked="" type="checkbox"/> Yes <input type="checkbox"/> No	(b) Restricted Information? <input checked="" type="checkbox"/> Yes <input type="checkbox"/> No
		(c) Restriction Type:	
(14) Clearance Review (Print/Sign): <i>J. D. Aardal / Janis Aardal</i>		Date: 01/04/2006	



# Modeling Data Package for an Initial Assessment of Closure of the C Tank Farm

R. Khaleel Fluor Government Group  
M.P. Connelly and W.J. McMahon CH2M HILL Hanford Group, Inc.  
Richland, WA 99352  
U.S. Department of Energy Contract DE-AC27-99RL14047

EDT/ECN: ~~NA~~ DRF UC:  
Cost Center: MF Charge Code:  
B&R Code: 1-4-06 Total Pages: 79

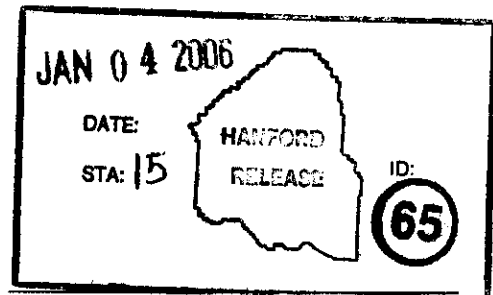
Key Words: modeling data package, impact assessment, tank farm closure, C tank farm

Abstract: As part of Hanford Site C tank farm closure, an initial impact assessment will be conducted to evaluate impacts on groundwater resources and long-term risk to human health. This report documents the data that will be used as input to estimate releases for various source terms and to perform subsequent flow and transport modeling through the vadose zone and the unconfined aquifer.

TRADEMARK DISCLAIMER. Reference herein to any specific commercial product, process, or service by trade name, trademark, manufacturer, or otherwise, does not necessarily constitute or imply its endorsement, recommendation, or favoring by the United States Government or any agency thereof or its contractors or subcontractors.

Printed in the United States of America. To obtain copies of this document, contact: Document Control Services, P.O. Box 950, Mailstop H6-08, Richland WA 99352, Phone (509) 372-2420; Fax (509) 376-4989.

*Janis Aardal* 01/04/06  
Release Approval Date



Release Stamp

Approved For Public Release



## **Modeling Data Package for an Initial Assessment of Closure of the C Tank Farm**

**R. Khaleel**  
Fluor Government Group

**M. P. Connelly**  
**W. J. McMahon**  
CH2M HILL Hanford Group, Inc.

**M. I. Wood**  
Fluor Hanford, Inc.

**Date Published**  
January 2006



Post Office Box 1500  
Richland, Washington

Prepared for the U.S. Department of Energy  
Office of River Protection

Contract # DE-AC27-99RL14047, Modification M030

**Approved for Public Release; Further Dissemination Unlimited**

## EXECUTIVE SUMMARY

As part of Hanford Site C tank farm closure, an initial impact assessment will be conducted to evaluate impacts on groundwater resources (i.e., the concentration of contaminants in groundwater) and long-term risk to human health (associated with groundwater use). The evaluations will consider the extent of contamination from residual wastes in tanks and tank ancillary equipment, past releases (i.e., tank leaks and spills), retrieval leaks, contaminant movement through the vadose zone to the saturated zone (groundwater), contaminant movement in the groundwater to various locations in groundwater, and the types of assumed human receptor activities at those locations.

For the reference analysis case, the source terms for the impact assessment consist of three separate sources that include past releases, tank residuals, and ancillary equipment residuals. This report documents the data that will be used as input to estimate releases for various source terms and to perform subsequent flow and transport modeling through the vadose zone and the unconfined aquifer. Contaminant species, representative of long-lived mobile radionuclides, will be considered for flow and transport modeling. All calculations will be performed on the basis of unit inventory and the results based on tank 241-C-112 will be scaled for the entire C waste management area. A spatial and temporal superposition will be used to obtain a composite contaminant breakthrough curve for releases due to residual wastes in tanks and tank ancillary equipment, past tank leaks and spills.

## CONTENTS

1.0	INTRODUCTION .....	1
1.1	SCOPE OF THIS DATA PACKAGE .....	1
2.0	OVERVIEW OF MODELING APPROACH .....	2
3.0	FACILITY DESCRIPTION AND GEOLOGY .....	6
3.1	FACILITY DESCRIPTION .....	6
3.2	GEOLOGY .....	6
4.0	RECHARGE RATES, AND FLOW AND TRANSPORT PARAMETERS.....	8
4.1	RECHARGE.....	8
4.2	FLOW AND TRANSPORT PARAMETERS.....	10
4.3	STOCHASTIC MODEL FOR MACROSCOPIC ANISOTROPY .....	10
4.3.1	Macroscopic Anisotropy Parameters .....	10
4.4	EFFECTIVE TRANSPORT PARAMETERS.....	11
4.4.1	Bulk Density and $K_d$ .....	11
4.4.2	Diffusivity .....	12
4.4.3	Macrodispersivity .....	12
5.0	GROUNDWATER FLOW AND TRANSPORT.....	13
5.1	FLOW AND TRANSPORT PARAMETERS.....	13
6.0	REFERENCES .....	14

## APPENDICES

A	WASTE MANAGEMENT AREA C CLOSURE NUMERIC CALCULATIONS.....	A-i
B	ADVECTION- AND DIFFUSION-DOMINATED RELEASE MODELS FOR RESIDUAL WASTES.....	B-i
C	GEOLOGIC CROSS-SECTION FOR C TANK FARM .....	C-i
D	WASTE MANAGEMENT AREA C VADOSE ZONE FLOW AND TRANSPORT PARAMETER ESTIMATES .....	D-i

## FIGURES

2-1.	Overall Modeling Approach for Risk Assessment .....	3
3-1.	Waste Management Area C and Surrounding Facilities .....	7

## TABLES

4-1.	C Tank Farm Recharge Estimates for Pre-Construction Period, Current Conditions, and Following Emplacement of Closure Barrier .....	9
4-2.	Composite van Genuchten-Mualem Parameters for Various Strata .....	10
4-3.	Macroscopic Anisotropy Parameters Based on Polmann (1990) Equations (Appendix D) for Various Strata .....	11
4-4.	Effective Parameter Estimates, $E[P_b K_d]$ , for Uranium for the Product of Bulk Density and $K_d$ .....	11
4-5.	Non-Reactive Macrodispersivity Estimates for Various Strata .....	12
5-1.	Transport Parameters from the Hanford Site-Wide Groundwater Model .....	14

## TERMS

### Abbreviations and Acronyms

$C_r$	Courant number
K	hydraulic conductivities
$K_d$	equilibrium linear sorption coefficient (distribution coefficient)
MUST	miscellaneous underground storage tank
$P_e$	Peclet number
RCRA	<i>Resource Conservation and Recovery Act of 1976</i>
SGM	site-wide groundwater model
WAC	<i>Washington Administrative Code</i>
WMA	waste management area
$\rho_b$	bulk density

### Units

%	percent
cm	centimeter
cm/s	centimeters per second
$\text{cm}^2/\text{s}$	square centimeters per second
$\text{cm}^3/\text{g}$	cubic centimeters per gram
ft	foot
$\text{g}/\text{cm}^3$	grams per cubic centimeter
gal	gallon
m	meter
$\text{mL}/\text{g}$	milliliters per gram
mm	millimeter
$\text{mm}/\text{yr}$	millimeters per year

## 1.0 INTRODUCTION

Under the *Hanford Federal Facility Agreement and Consent Order* (Ecology et al. 1989), both single-shell tanks and double-shell tanks are *Resource Conservation and Recovery Act of 1976* (RCRA) hazardous waste management units that will eventually be closed under *Washington Administrative Code* (WAC) 173-303, “Dangerous Waste Regulations.” The closure options under review are: 1) clean closure, involving removal of all waste and waste constituents, including tanks, debris, contaminated equipment, and contaminated soil and groundwater; 2) modified closure, which involves a variety of closure methods but requires periodic (at least once after five years) assessments to determine if modified closure requirements are being met; and 3) closure as a landfill with waste remaining in place and corrective action taken for contaminated media under post-closure requirements. All three options require the submittal of closure plans and their approval by Washington State Department of Ecology. As stated below, tank closure options are under review.

The clean closure option risk assessment is being evaluated as part of the *Environmental Impact Statement for Retrieval, Treatment, and Disposal of Tank Waste and Closure of Single-Shell Tanks at the Hanford Site, Richland, WA...* It is anticipated that the clean closure option (e.g., excavating and removing all 149 SSTs, along with contaminated soil and disposing of this material) will not be feasible for the SSTs and that the WMAs that contain the SSTs will be closed as landfills. (*Single-Shell Tank System Closure Plan* [Lee 2004, p. 4-1]).

Therefore, for the purpose of this initial assessment, it is assumed that waste management area (WMA) C will be closed as landfill. The objective of this report is to document the data that will be used as input to perform preliminary flow and transport modeling through the vadose zone and the unconfined aquifer for closure of WMA C in the 200 East Area. Calculations will be performed based on unit inventory for various contaminant source terms, and the modeling results based on tank 241-C-112 will be scaled for other tanks in the C tank farm.

### 1.1 SCOPE OF THIS DATA PACKAGE

The following information is included as part of the scope for this data package for the modeling:

- Modeling approach (Section 2.0)
- Numerical cases to be run (Appendix A)
- Source-term release scenarios for release of residual waste contaminants from tanks (Appendix B)
- Facility description and stratigraphic cross-sectional models for C tank farm (Section 3.0 and Appendix C)
- Recharge (infiltration) data for C tank farm (Section 4.0)
- Effective (upscaled) moisture retention, saturated and unsaturated hydraulic conductivity, bulk density, diffusivity, and macrodispersivity estimates for various strata (Section 4.0 and Appendix D)
- Macrodispersivity estimates for selected radionuclide species (Section 4.0 and Appendix D)
- Groundwater flow and transport parameters (Section 5.0).

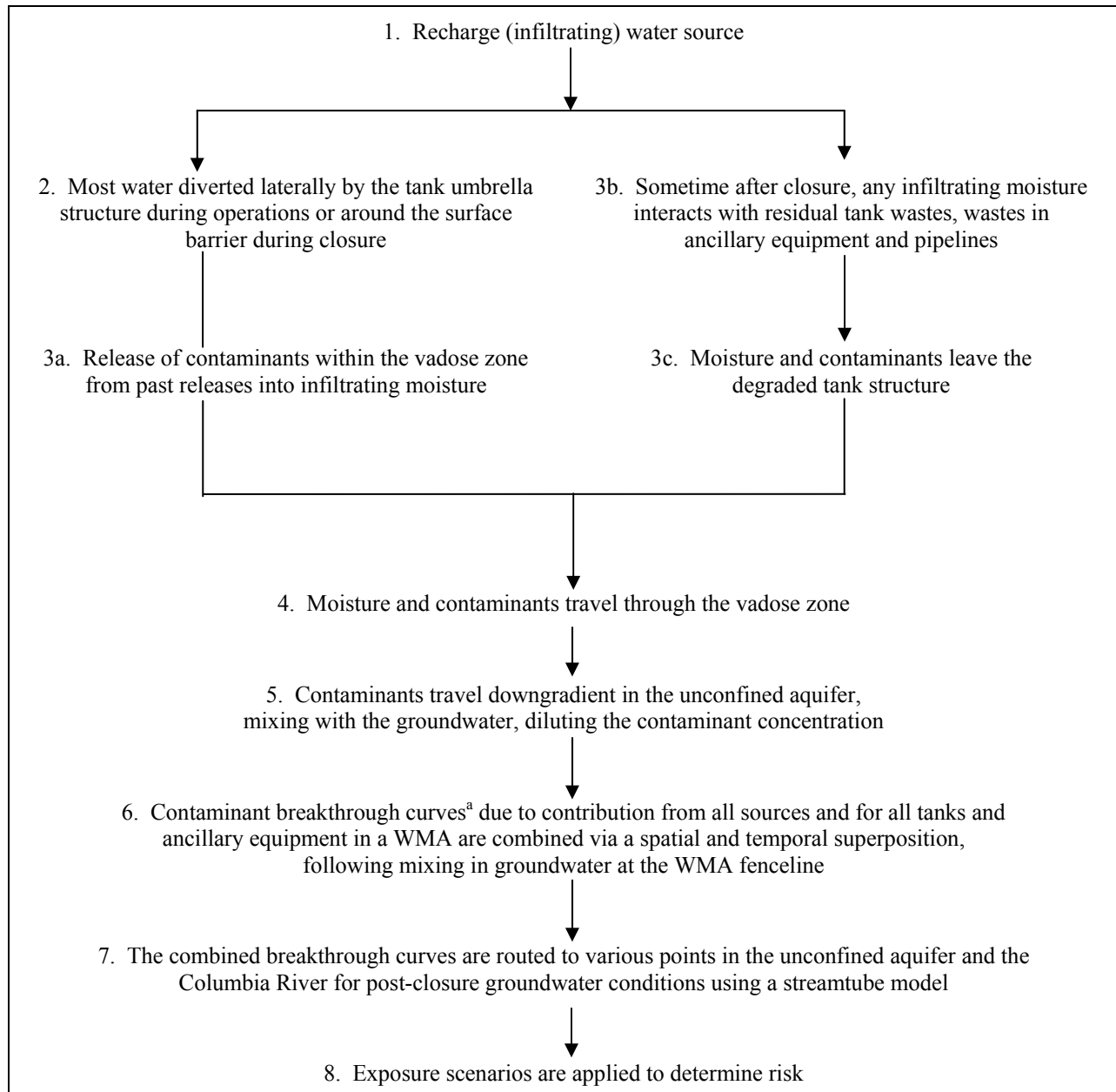
## 2.0 OVERVIEW OF MODELING APPROACH

The source terms for the initial assessment consist of three separate sources that include past releases, tank residuals, and ancillary equipment residuals. The past releases represent tank leaks and spills which have leaked into the vadose zone and have migrated through the vadose zone for a number of years. Releases from the residual wastes (both from tank and tank ancillary equipment) would typically occur over an extended period following closure of the tank farm when infiltrating water would enter the tank or tank ancillary equipment, dissolve contaminants, and migrate into the vadose zone and to the groundwater.

The overall modeling approach for the groundwater pathway is illustrated in Figure 2-1. The modeling considers the extent of contamination from the following sources and processes:

- Residual waste in tanks
- Tank ancillary equipment (i.e., pipelines and miscellaneous underground storage tanks [MUST])
- Past releases (i.e., tank leaks and unplanned releases or spills)
- Contaminant movement through the vadose zone to the saturated zone (groundwater)
- Contaminant movement in the groundwater to various calculation points
- Assumed human receptor activities at the WMA fenceline.

As indicated in Figure 2-1, the model assumed that infiltration of moisture from precipitation eventually enters the WMA (step 1), but most of the water is diverted around the tank structure during operations or around the surface barrier during closure (step 2). During the tank farm operational period, contaminants released within the vadose zone from past releases are driven by the infiltrating moisture (step 3a). Following closure, contaminants are released into the vadose zone from the degraded tank structure and ancillary equipment by contact with recharge water (steps 3b and 3c). The infiltrating water, along with contaminants from past releases and residual wastes from steps 2 and 3, travels through the vadose zone (step 4). The contaminants from all sources travel through the vadose zone until they reach the water table and the unconfined aquifer (step 5). The contaminant breakthrough curves from residual wastes and past releases are combined via a spatial and temporal superposition (step 6). The combined breakthrough curves are then routed to various locations within the unconfined aquifer and the Columbia River, using an analytical solution (i.e., streamtube model) (step 7). In the final step of the modeling, the exposure scenario risk factors are applied to estimated groundwater concentrations to determine risk (step 8).

**Figure 2-1. Overall Modeling Approach for Risk Assessment**

<sup>a</sup> Contaminant breakthrough curves provide the concentration versus time history.

Two-dimensional simulations yield the contaminant mass flux and breakthrough curves at the tank farm fenceline along the tank centerlines for the selected cross-section. The tank centerline mass flux and breakthrough curves are transformed to average values across the WMA fenceline based on results of three-dimensional simulations (Appendix A).

The strategy for the simulations performed for WMA C (including tanks, waste transfer pipelines, leak detection systems, and MUSTs) was to define and analyze both a reference analysis case and a suite of sensitivity/“what if” cases (Appendix A). The reference analysis

case was developed using the best available information for the physical system and the WMA C facilities, and the closure plans for this WMA. Sensitivity/“what if” cases were defined to explore the relative impact of uncertainties in models, data, and assumptions on the estimated impacts.

All calculations are for a single tank (i.e., tank 241-C-112 in C tank farm) and for unit curie (or unit mass) as a source term for each of the three sources (i.e., past leaks, tank residuals, and ancillary equipment residuals). Wastes currently residing in the vadose zone due to past leaks and spills are distributed over varying dimensions and depths. Release rates of contaminants within the vadose zone are dependent on contaminant-specific sorption and solubility reactions. For the past tank leak simulations, the following simplifying assumptions were made:

- One homogeneous contaminant distribution over one waste volume size and depth interval (based on field data from recently drilled boreholes) is assumed for all past releases within WMA C.
- The entire leaked inventory is readily available for transport with the infiltrating water where transport is only limited by the chemical adsorption to the soils.

The final tank residual waste configuration and inventories will be dependent on the waste retrieval practices that remain to be applied to the Hanford Site waste tanks. Also, the release mechanisms for contaminants from the closed tanks are currently not known. For the simulations, the following assumptions have been made for the contaminant release from residual waste for the reference analysis case:

- Contaminant migration from residual wastes in the tanks and MUSTs is dominated by diffusional processes
- An analytical model for diffusion was used for residual waste contaminants released from tanks and MUSTs (neglecting tank structure details and any future cracking that may occur within the system)
- Contaminant-specific sorption and solubility were not modeled
- The source location for the contaminant release from tanks and MUSTs was assumed to be directly beneath the tank.

The final residual waste configuration and inventories will be dependent on the actual retrieval of residual wastes from the ancillary equipment. Also, the release mechanisms for contaminants from the closed ancillary equipment are currently not known. For the simulations, the following assumptions are made for the contaminant release from the pipelines:

- Residual waste contaminants within the pipelines are assumed to be readily available for transport with the infiltrating water.
- The distribution of tank ancillary equipment within the WMA is ignored. The location of inventories for pipelines in the numerical simulations is assumed to be represented by a homogeneous distribution at a depth of 8 m (25 ft) and extending horizontally for 8 m (25 ft). Further details are provided in Appendix A.

Two-dimensional flow and transport models along a row of tanks will be used for all vadose zone simulations. Steady-state initial conditions will be developed by simulating from a unit hydraulic gradient condition to a steady-state condition, dictated by the initial meteoric recharge at the surface, water table elevation, water table gradient, no flux vertical boundaries, variation of hydrologic properties, and location of impermeable tanks.

The steady-flow simulation, representing flow conditions up to the year when tank farm construction is completed (i.e., 1945 for the C tank farm), will be used as the initial condition for all subsequent operational period flow simulations. Transient flow conditions will be simulated from the year of construction to the year 2000. Transient flow and contaminant transport simulations begin in the year 2000 and end after a 10,000-year assessment period beyond closure of the tank farm in year 2032 (i.e., years 2032 to 12032). Transient conditions involve changes in the flow fields in response to current conditions, placement of closure barrier, and effects of a degraded barrier. The recharge estimates for various times are described in Section 4.0. For simulating the time period prior to construction of C tank farm (Table 4-1), the pre-construction material is H1 (gravelly sand) (Section 3.0). After construction in 1945, the material is backfill.

All simulations will be run assuming isothermal conditions. The vadose zone will be modeled as an aqueous-gas porous media system where transport through the gas phase is neglected.

Fluid flow within the vadose zone will be described by Richards' equation (Domenico and Schwartz 1990, *Physical and Chemical Hydrogeology*), whereas the contaminant transport will be described by the conventional advective-dispersive transport equation with an equilibrium linear sorption coefficient ( $K_d$ ) formulation. A series of mobile to moderately retarded contaminant species ( $K_d = 0, 0.02, 0.1, 0.2, 0.6, 1.0, 2.0, \text{ and } 5.0 \text{ mL/g}$ ) will be considered for each run.

The geologic strata are assumed continuous but not of constant thickness. A detailed stratigraphic cross-sectional model for the C tank farm is presented in Appendix C; the model includes the effect of dipping strata. The enhanced spreading at the fine-grained/coarse-grained interfaces and the increased downdip movement of the plume along these interfaces are included in the model. The simulation domain will be extended horizontally to make certain that the prescribed boundary conditions are not violated. Uniform Cartesian grid spacing specified in input files will be used to model geologic features.

No site-specific data are available on soil moisture characteristics for the C tank farm. Data catalogs are, however, available for 200 Area soils. For this work, data on laboratory measurements for moisture retention, particle-size distribution, saturated and unsaturated hydraulic conductivity, and bulk density for individual stratum are based on data for similar soils in the 200 East and 200 West Areas (Khaleel et al. 2000, *Modeling Data Package for S-SX Field Investigation Report (FIR)*). For each stratum defined by the stratigraphic cross-sectional model, the small-scale laboratory measurements are upscaled to obtain equivalent horizontal and vertical unsaturated hydraulic conductivities as a function of mean tension, as shown in Khaleel et al. (2000). Khaleel et al. (2002a), "Upscaled Flow and Transport Properties for Heterogeneous Unsaturated Media," and Khaleel et al. (2002b), "Effective Hydraulic Conductivity and Macrodispersivity Estimates for Heterogeneous Unsaturated Media," show that upscaling of unsaturated hydraulic conductivities ( $K$ ) leads to development of macroscopic

anisotropies (as a function of mean tension) for each layer (Section 5.0 and Appendix D). An averaging of van Genuchten parameters ( $\theta_r$ ,  $\theta_s$ ,  $\alpha$ , and  $n$ ) (van Genuchten 1980, “A Closed-Form Solution for Predicting the Conductivity of Unsaturated Soils”) is used to define a moisture retention curve for each stratum (Section 5.0 and Appendix D).

In case multiple samples are not available for each stratum, data from other sites in the 200 Areas are used. Attempts are made to use hydraulic properties that were obtained using both laboratory-measured moisture retention and unsaturated hydraulic conductivity. This is primarily to avoid extrapolating the unsaturated conductivities (van Genuchten 1980; Mualem 1976, “A New Model Predicting the Hydraulic Conductivity of Unsaturated Porous Media”) to the dry end, based only on saturated conductivity estimate (Khaleel et al. 1995, “Evaluation of van Genuchten-Mualem Relationships to Estimate Unsaturated Conductivity at Low Water Contents”). In addition, to reflect field conditions, the laboratory data will be corrected for the presence of any gravel fraction in the sediment samples (Khaleel and Relyea 1997, “Correcting Laboratory-Measured Moisture Retention Data for Gravels”). As with flow modeling, each stratum is modeled with different transport parameters (i.e., bulk density, diffusivity, and dispersivity). The aquifer hydraulic conductivity is 3,000 m/day, the gradient is  $1.1 \times 10^{-3}$ , and the porosity is 0.25.

An analytical/streamtube approach will be used to model groundwater flow and transport. The analytical solution in Domenico and Schwartz (1990) or any comparable analytical/streamtube model can be used to model saturated transport.

A description of the cases to be modeled is presented in Appendix A.

### **3.0 FACILITY DESCRIPTION AND GEOLOGY**

#### **3.1 FACILITY DESCRIPTION**

The C farm tanks were built during the initial 30-month war time construction period (1943 to 1944) in the 200 East Area, near the location of the planned C Plant chemical processing facility. The C tank farm consists of 12 100-Series tanks and 4 200-Series tanks (Figure 3-1). The 100-Series tanks are 22.9 m (75 ft) in diameter with capacities of 2,010,000 L (530,000 gal). The 200-Series tanks are 6.1 m (20 ft) in diameter with capacities of 208,000 L (55,000 gal). Both types of tanks are constructed of reinforced concrete with welded carbon steel liners (Wood et al. 2003).

#### **3.2 GEOLOGY**

A detailed discussion of C tank farm geology, including the cross-section to be used for modeling, is provided in Appendix C. There are several sedimentary sequences overlying the basalt beneath the C tank farm. These are, from top to bottom:

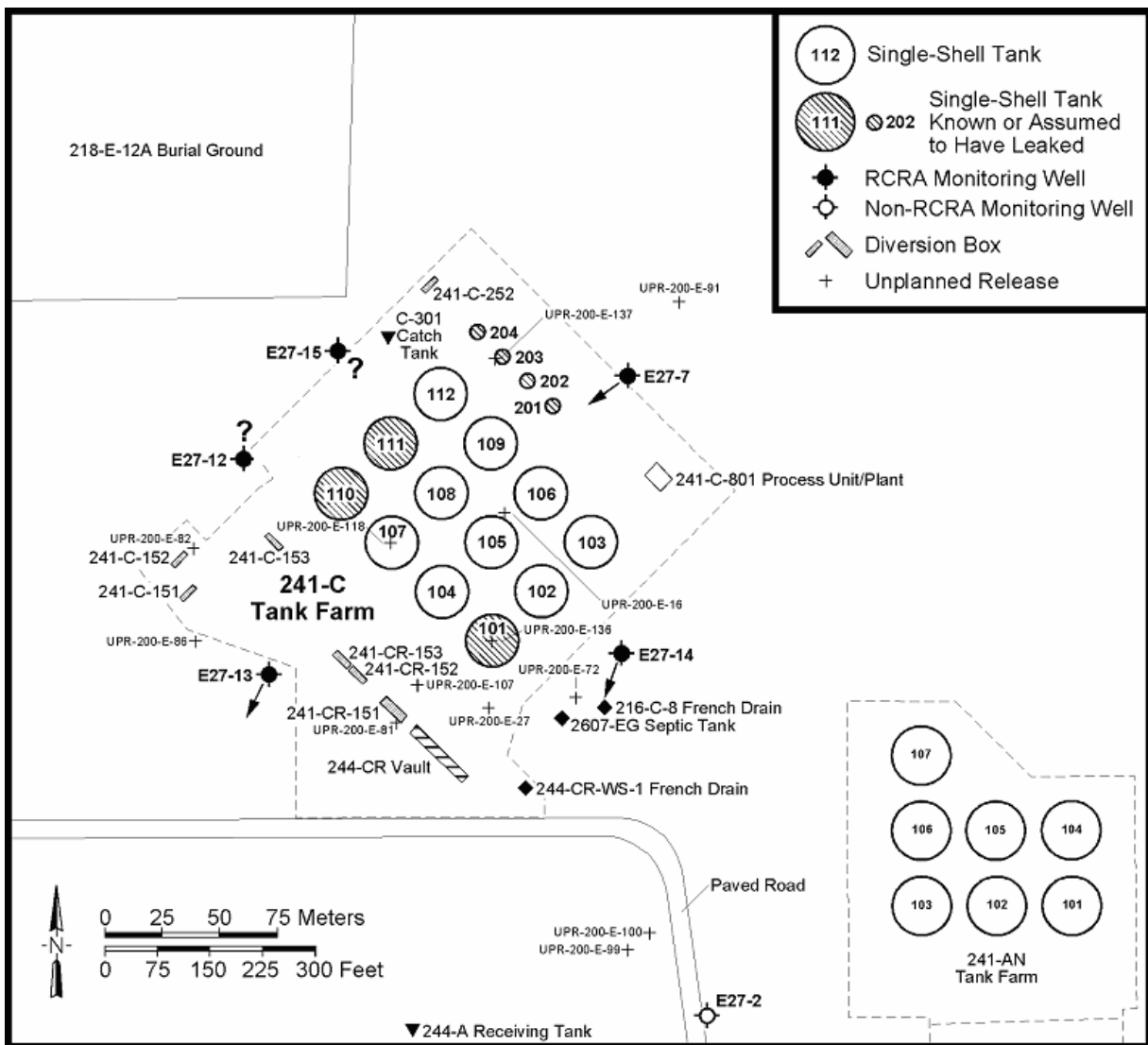
- Backfill (material type 1, sandy gravel)
- Hanford formation – upper gravelly sequence (H1 unit, material type 4, gravelly sand)
- Hanford formation – sand sequence (H2 unit, material type 2, sand)
- Hanford formation – lower gravelly sequence (H3 unit, material type 3, gravelly sand)

- Undifferentiated Cold Creek unit (pre-Missoula Gravels) and/or Ringold Formation UnitA? [material type 5].

The geologic strata are assumed to be continuous but not of constant thickness. The inclination for individual strata, whenever tilted, can be approximated from the cross-sections shown in Figure C-1 in Appendix C. Note that, in some cases, a single slope will not be enough to represent the incline for individual strata. For example, several segments will be needed to approximate the material type 3 in Figure C-1. The water table is located approximately 79 m (259 ft) below ground surface. The hydraulic and transport properties to be used for the sedimentary sequences in the flow and transport modeling are given in Section 4.0.

For the sensitivity/“what if” case assuming advective contaminant release from the tank waste residuals (Appendix A), the fill material for the tanks, following tank degradation, will be backfill (material type 1, sandy gravel).

**Figure 3-1. Waste Management Area C and Surrounding Facilities**



## 4.0 RECHARGE RATES, AND FLOW AND TRANSPORT PARAMETERS

The purpose of this section is to present available data on surface infiltration (recharge). Also presented are effective (upscaled) flow and transport parameters. The effective parameters are based on laboratory measurements for moisture retention, saturated and unsaturated hydraulic conductivity, and bulk density for sediment samples that are similar in particle size distribution to WMA C sediment samples. Parameters are provided for the reference analysis case and the sensitivity/“what if” cases described in Appendix A.

### 4.1 RECHARGE

Recharge is the amount of water reaching the unconfined aquifer after evapotranspiration (loss through evaporation and transpiration of plants). Deep aquifer recharge cannot be measured directly. It is estimated by measuring infiltration using field lysimeters and via modeling studies. Tank farm surfaces are covered with gravel to prevent growth of vegetation and provide radiation shielding for site workers. Bare gravel surfaces, however, enhance net recharge of meteoric water, compared to undisturbed naturally vegetated surfaces. Recharge is further enhanced in tank farms by the effect of percolating water being diverted by the impermeable, sloping surface of the tank domes. This umbrella effect is created by the 23-m diameter buried tank domes. Water, shed from the tank domes, flows down the tank walls into underlying sediments. Sediments adjacent to the tanks, while remaining unsaturated, can attain elevated moisture contents. Enhanced recharge from a gravel-covered tank dome can provide potential for faster transport of contaminants to the water table.

Recharge can vary greatly depending on factors such as climate, vegetation, surface condition, and soil texture. Studies conducted over the last decade at the Hanford Site, such as Gee et al. (1992), “Variations in Recharge at the Hanford Site,” suggest that recharge rates can vary from less than 0.1 mm/yr on a variety of soil and vegetative combinations to greater than 130 mm/yr on bare basalt outcrops or bare, gravel-covered waste sites. Data from experimental sites such as the Field Lysimeter Test Facility and the Prototype Hanford Barrier, both in the 200 Area, suggest that recharge through gravels can vary from 15 to 70% of precipitation, with the lower amount occurring under vegetated conditions (Gee et al. 1996, *Hanford Prototype Barrier Status Report FY 1996*; Fayer and Walters 1995, *Estimated Recharge Rates at the Hanford Site*; Fayer et al. 1996, “Estimating Recharge Rates for a Groundwater Model Using a GIS”). With a long-term annual average precipitation of 160 mm, the higher percentage translates into a recharge rate of about 100 mm/yr that was observed on clean gravels that were kept free of vegetation (Fayer et al. 1999, *Recharge Data Package for the Immobilized Low Activity Waste 2001 Performance Assessment*). Drainage from bare sands is about 55 mm/yr (Fayer and Walters 1995) to about 70 mm/yr under Hanford Site climatic conditions (Ward et al. 1997, *A Comprehensive Analysis of Contaminant Transport in the Vadose Zone Beneath Tank SX-109*). There has been no direct measurement of recharge for tank farm gravels, which are known to contain a larger amount of fines than the clean gravels. Thus, it is entirely possible that the tank farms experience a recharge rate that ranges between the estimate for bare sand and the estimate for gravels (Ward et al. 1997). For the purpose of this work, a reference case recharge estimate of 100 mm/yr will be used prior to closure (Table 4-1).

**Table 4-1. C Tank Farm Recharge Estimates for Pre-Construction Period, Current Conditions, and Following Emplacement of Closure Barrier**

Condition Simulated	Recharge Estimate (mm/yr)	Duration	Comment
Before construction of C tank farms, the construction period being 1943 to 1944	3.5	Until steady state moisture conditions are achieved for the year 1945	Vadose zone flow simulated at the recharge rate of 3.5 mm/yr to develop initial moisture conditions for subsequent simulations
Current conditions	100 <sup>a</sup>	1945 to 2032	Recharge is assumed to increase from the pre-construction period estimate of 3.5 mm/yr to the current value of 100 mm/yr. <sup>b</sup> During this period, the ground cover is gravel with no vegetation. An enhanced RCRA Subtitle C barrier is assumed to be in place by 2032.
Transition to conditions of restricted recharge due to enhanced RCRA Subtitle C barrier	0.5	2032 to 2532	Recharge is assumed to decrease from a current estimate of 100 mm/yr to the barrier design value of 0.5 mm/yr. The barrier is assumed to function to its design estimate of 500 years. <sup>b</sup>
Degraded barrier condition	1.0	2532 to 12032	The barrier is degraded and recharge increases from 0.5 mm/yr to 1.0 mm/yr until the end of simulation at year 12032. <sup>b</sup>

<sup>a</sup> Based on 8-year lysimeter data for graveled surface (Fayer et al.1999).

<sup>b</sup> Appropriate transition periods, as needed, can be used to accommodate the sharp breaks in individual recharge estimates.

The closure barrier for tank farms is assumed to be an enhanced RCRA Subtitle C barrier with a design life of 500 years; the recharge for such a barrier is estimated to be 0.1 mm/yr (Fayer et al. 1999). For the initial assessment calculations, a higher recharge of 0.5 mm/yr will be used since the barrier for this WMA has not yet been designed. The 0.5 mm/yr estimate is the design objective for this type of barrier described in *Permanent Isolation Surface Barrier Development Plan*, Wing (1994). For a degraded closure barrier, recharge rates are expected to increase to a recharge estimate of 1.0 mm/yr for the reference analysis case.

Table 4-1 summarizes the timeline estimates for barrier emplacement at the C tank farm and the corresponding recharge estimates.

For the tank farm cross-sections, the numerical simulation cases identified in Appendix A will have an assessment period beginning January 1, 2000 and continuing for 10,000 years beyond closure of the tank farm in year 2032 (i.e., ending in year 12032). It is assumed that a closure barrier will be in place by 2032. In cases where credit is taken for barrier integrity, it is assumed that a closure barrier will function as designed for 500 years.

For numerical simulations, the initial moisture contents (and the initial matric suctions) for the flow domain will be established by allowing the vadose zone model to equilibrate with a recharge rate representative of natural recharge for the tank farm location.

## 4.2 FLOW AND TRANSPORT PARAMETERS

This section provides effective (upscaled) values of flow and transport parameters for the vadose zone. Specific flow parameters include moisture retention, and saturated and unsaturated hydraulic conductivity. Transport parameters include bulk density, diffusivity, sorption coefficients, and macrodispersivity. Details on deriving the effective (upscaled) parameters are addressed in Appendix D.

Table 4-2 lists the composite, fitted van Genuchten-Mualem (van Genuchten 1980; van Genuchten et al. 1991, *The RETC Code for Quantifying the Hydraulic Functions of Unsaturated Soils*) parameters for various strata. Again, note that the material types noted in Table 4-2 (and elsewhere) are identical to those in Appendix C, Figure C-1. Estimates for the equivalent horizontal and vertical hydraulic conductivities are presented in the Section 4.3.

**Table 4-2. Composite van Genuchten-Mualem Parameters for Various Strata**

Strata/Material Type	Number of Samples	$\theta_s$	$\theta_r$	$\alpha$ 1/cm	n	$\ell$	Fitted $K_s$ cm/s
Backfill (1)	10	0.1380	0.0100	0.0210	1.374	0.5	5.60E-04
Sand H2 (2)	12	0.3819	0.0443	0.0117	1.6162	0.5	9.88E-05
Gravelly Sand H3 (3)	8	0.2688	0.0151	0.0197	1.4194	0.5	5.15E-04
Gravelly Sand H1 (4)	11	0.2126	0.0032	0.0141	1.3730	0.5	2.62E-04
Cold Creek unit (pre-Missoula Gravels)/ Ringold Sandy Gravel (5)	10	0.1380	0.0100	0.0210	1.374	0.5	5.60E-04

See Appendix D for a description of the variables.

## 4.3 STOCHASTIC MODEL FOR MACROSCOPIC ANISOTROPY

As discussed in Appendix D, variable, tension-dependent anisotropy provides a framework for upscaling small-scale measurements to the effective (upscaled) properties for the large-scale vadose zone. A stochastic model (Polmann 1990, *Application of Stochastic Methods to Transient Flow and Transport in Heterogeneous Unsaturated Soils*) is used to evaluate tension dependent anisotropy for sediments at the C tank farm; details are in Appendix D. Note that Polmann (1990) parameters (Table 4-3) will only be used to assign anisotropy ratios for various strata within the vadose zone.

### 4.3.1 Macroscopic Anisotropy Parameters

Table 4-3 lists the variable, macroscopic anisotropy parameter estimates for various strata at WMA C. Details on derivation of the parameter estimates are in Appendix D.

**Table 4-3. Macroscopic Anisotropy Parameters Based on Polmann (1990) Equations (Appendix D) for Various Strata**

Strata/Material Type	Number of Samples	$\langle \text{Ln}K_s \rangle$	$\sigma_{\text{Ln}K_s}^2$	p	$\zeta$	$\lambda$ cm	A
Backfill (1)	10	-15.76	3.56	-1.1E-04	1.84E-04	30	0.00371
Sandy H2 (2)	12	-14.59	1.50	-7.2E-04	6.55E-04	50	0.00620
Gravelly Sand H3 (3)	8	-15.30	1.83	-5.6E-04	5.16E-04	50	0.00415
Gravelly Sand H1 (4)	11	-14.85	1.94	-2.6E-04	2.50E-04	30	0.00368
Cold Creek unit (pre-Missoula Gravels)/Ringold Sandy Gravel (5)	10	-15.76	3.56	-1.1E-04	1.84E-04	30	0.00371

See Appendix D for a description of the variables.

#### 4.4 EFFECTIVE TRANSPORT PARAMETERS

Reference case effective transport parameter (i.e., bulk density, diffusivity, and dispersivity) estimates are presented in this section. Because of natural variability, the transport parameters are all spatially variable. The purpose is again, similar to the flow parameters, to evaluate the effect of such variability on the large-scale transport process.

##### 4.4.1 Bulk Density and $K_d$

Both bulk density ( $\rho_b$ ) and  $K_d$  estimates are needed to calculate retardation factors for different species. The effective, large-scale estimate for the product  $[\rho_b K_d]$  is the average of the product of small-scale laboratory measurements for bulk density and  $K_d$  (Gelhar 1993, *Stochastic Subsurface Hydrology*). A series of mobile to moderately retarded contaminant species ( $K_d = 0, 0.02, 0.1, 0.2, 0.6, 1.0, 2.0,$  and  $5.0$  mL/g) will be considered for each run. Table 4-4 provides the effective, large-scale estimates for uranium as an example contaminant.

The average  $\rho_b$ ,  $E[\rho_b]$  (Table 4-4) estimates are based on data in Tables D-1 through D-4 of Appendix D for various strata. The  $K_d$  estimates (Table 4-4) for uranium are based on data for undisturbed sediments from Kaplan and Serne (2000), *Geochemical Data Package for the Immobilized Low-Activity Waste Performance Assessment*. Calculations (Table 4-4) for  $E[\rho_b]$  and  $E[\rho_b K_d]$  for uranium include correction for the gravel fraction.

**Table 4-4. Effective Parameter Estimates,  $E[\rho_b K_d]$ , for Uranium for the Product of Bulk Density and  $K_d$**

Strata/Material Type	$K_d$ cm <sup>3</sup> /g	$E[\rho_b]$ g/cm <sup>3</sup>	$E[\rho_b K_d]$
Backfill (1) and Cold Creek unit (pre-Missoula Gravels)/Ringold Gravels (5)	0.6	2.13	0.59
Sandy H2 (2)	0.6	1.76	1.04
Gravelly sand H3 (3)	0.6	1.94	1.17
Gravelly sand H1 (4)	0.6	2.07	1.24

See Appendix D for a description of the variables.

#### 4.4.2 Diffusivity

It is assumed that the effective, large-scale diffusion coefficients for all strata at the C tank farm are a function of volumetric moisture content,  $\theta$ , and can be expressed using the Millington and Quirk (1961), “Permeability of Porous Solids,” empirical relation:

$$D_e(\theta) = D_0 \frac{\theta^{10/3}}{\theta_s^2} \quad \text{Equation 1}$$

where  $D_e(\theta)$  is the effective diffusion coefficient of an ionic species as a function of moisture content, and  $D_0$  is the effective diffusion coefficient for the same species in free water. The molecular diffusion coefficient for all species in free water is assumed to be  $2.5 \times 10^{-5} \text{ cm}^2/\text{s}$  (Kincaid et al. 1995, *Performance Assessment of Grouted Double-Shell Tank Waste Disposal at Hanford*).

#### 4.4.3 Macrodispersivity

An extended review is provided in Appendix D on the rationale for vadose zone macrodispersivity estimates. Macrodispersivity estimates are needed for both reactive (i.e., uranium) and non-reactive (i.e., technetium-99) species.

##### 4.4.3.1 Macrodispersivity Estimates for Non-Reactive Species

Macrodispersivity estimates for non-reactive species (i.e., technetium-99) are listed in Table 4-5. Again, details on basis for the estimates are provided in Appendix D.

**Table 4-5. Non-Reactive Macrodispersivity Estimates for Various Strata**

Strata/Material Type	$\sigma_{LnK}^2$	Correlation length, $\lambda$ cm	$A_L$ cm	$A_T$ cm
Backfill (1) and Cold Creek unit (pre-Missoula Gravels)/Ringold Sandy Gravel (5)	4.54	30	~150	15
Sandy H2 (2)	4.60	30	~150	15
Gravelly sand H3 (3)	4.95	30	~100	10
Gravelly sand H1 (4)	3.19	30	~100	10

See Appendix D for a description of the variables.

##### 4.4.3.2 Heterogeneous Sorption Enhanced Macrodispersivities for the Reactive Species

As expected, the net effect of sorption is to retard the velocity of the contaminant. Because sorption for specific contaminants may be a function of soil properties, as the soil properties experience spatial variability, the sorption also varies (Gelhar 1993; Talbott and Gelhar 1994, *Performance Assessment of a Hypothetical Low-Level Waste Facility: Groundwater Flow and Transport Simulation*).

Stochastic analysis results for macrodispersivity enhancement for various strata are shown in Table D-9 of Appendix D for the reactive species (i.e., uranium). Note that the unsaturated K values were evaluated at -100 cm via the fitted van Genuchten-Mualem relation.

The macrodispersivity enhancement ranged from about 1.06 for the H2 sandy sediments to about 1.12 for the H1 gravelly sand sediments (Appendix D).

#### 4.4.3.3 Numerical Considerations

A complicating factor in numerical modeling of contaminant transport in porous media is that both finite-difference and finite-element solutions are affected by “numerical dispersion,” which refers to artificial dispersion caused by errors associated with discretization of the flow domain. To minimize such errors, the grid should be designed so that the Peclet number ( $P_e = \text{discretized distance/dispersivity}$ ) is less than or equal to one, although acceptable solutions can be obtained with  $P_e$  as high as 10 (Huyakorn and Pinder 1983, *Computational Methods in Subsurface Flow*). With low dispersivities within the vadose zone, the Peclet number criterion results in grid spacings that are not very practical to implement. This is why numerical modelers often resort to higher values of dispersivity. An alternative is to consider use of an “upwinding” option to control numerical dispersion (Huyakorn and Pinder 1983).

Another consideration is discretization of simulation time so that the Courant number ( $C_r = \text{pore velocity} \times \text{time interval/grid spacing}$ ) is less than or equal to one. That is, the time step should be selected so that the chosen time interval is less than the value obtained by the ratio of grid spacing to pore velocity. Thus, the time step should be selected so that it is less than the time it takes for the solute to move one grid spacing. Note that, for a three-dimensional problem, the  $P_e$  and  $C_r$  criteria are applicable to transport in all three directions.

## 5.0 GROUNDWATER FLOW AND TRANSPORT

### 5.1 FLOW AND TRANSPORT PARAMETERS

The Hanford Site-wide groundwater model (SGM) is used to assign the flow properties such as effective porosity, saturated hydraulic conductivity, and hydraulic gradient of the unconfined aquifer for the vadose zone model (Wurstner et al. 1995, *Development of a Three-Dimensional Ground-water Model of the Hanford Site Unconfined Aquifer System, FY 1995 Status Report*; Cole et al. 2001, *Transient Inverse Calibration of Hanford Site-Wide Groundwater Model to Hanford Operational Impacts - 1943 to 1996*). See Table 5-1, and Appendix A, Tables A-1 and A-2 for depth to water table, hydraulic conductivity, hydraulic gradient, and effective porosity.

Beyond the fenceline of WMA C, an analytical/streamtube methodology will be used to model groundwater flow and transport. The analytical solution in Domenico and Schwartz (1990) or any comparable analytical/streamtube model can be used to model saturated transport. Information on flow and transport properties needed for the analytical/streamtube model is based on parameters in the SGM (Wurstner et al. 1995; Cole et al. 2001). The SGM is used to estimate the steady-state post-Hanford Site operations water table, hydraulic gradient, and flow velocities near WMA C and in the 200 Areas. All parameters needed for the streamtube model application are given in Table 5-1.

**Table 5-1. Transport Parameters from the Hanford Site-Wide Groundwater Model <sup>a</sup>**

Parameter	Estimate
Longitudinal macrodispersivity	62.5 m
Lateral macrodispersivity	12.5 m
Vertical macrodispersivity	0.0002 m
Diffusion coefficient <sup>b</sup>	$2.5 \times 10^{-5}$ cm <sup>2</sup> /sec
Distribution coefficient (K <sub>d</sub> )	Varies by contaminant
Depth to water table	79 m (259 ft)
Hydraulic gradient	0.00001
Hydraulic conductivity (K <sub>sat</sub> )	3,000 m/day
Effective porosity	0.25

<sup>a</sup> Based on Wurstner et al. (1995) and Cole et al. (2001) unless noted.

<sup>b</sup> Kincaid et al. (1995)

## 6.0 REFERENCES

- Cole, C.R., M.P. Bergeron, S.K. Wurstner, P.D. Thorne, S. Orr, and M.I. McKinley, 2001, *Transient Inverse Calibration of Hanford Site-Wide Groundwater Model to Hanford Operational Impacts - 1943 to 1996*, PNNL-13447, Pacific Northwest National Laboratory, Richland, Washington.
- Domenico, P.A., and F.W. Schwartz, 1990, *Physical and Chemical Hydrogeology*, John Wiley, New York, New York.
- Ecology, EPA, and DOE, 1989, *Hanford Federal Facility Agreement and Consent Order*, as amended, Washington State Department of Ecology, U.S. Environmental Protection Agency, and U.S. Department of Energy, Olympia, Washington.
- Fayer, M.J., and T.B. Walters, 1995, *Estimated Recharge Rates at the Hanford Site*, PNL 10285, Pacific Northwest Laboratory, Richland, Washington.
- Fayer, M.J., E.M. Murphy, J.L. Downs, F.O. Khan, C.W. Lindenmeier, and B.N. Bjornstad, 1999, *Recharge Data Package for the Immobilized Low-Activity Waste 2001 Performance Assessment*, PNNL-13033, Pacific Northwest National Laboratory, Richland, Washington.
- Fayer, M.J., G.W. Gee, M.L. Rockhold, M.D. Freshley, and T.B. Walters, 1996, "Estimating Recharge Rates for a Groundwater Model Using a GIS," *J. Environ. Qual.*, Vol. 25, pp. 510-518.
- Gee, G.W., A.L. Ward, B.G. Gilmore, S.O. Link, G.W. Dennis, and T.K. O'Neil, 1996, *Hanford Prototype Barrier Status Report FY 1996*, PNNL-11367, Pacific Northwest National Laboratory, Richland, Washington.

- Gee, G.W., M.J. Fayer, M.L. Rockhold, and M.D. Campbell, 1992, "Variations in Recharge at the Hanford Site," *Northwest Sci.*, Vol. 66, pp. 237-250.
- Gelhar, L.W., 1993, *Stochastic Subsurface Hydrology*, Prentice Hall, New York.
- Huyakorn, P.S., and G.F. Pinder, 1983, *Computational Methods in Subsurface Flow*, Academic Press, New York.
- Kaplan, D.L., and R.J. Serne, 2000, *Geochemical Data Package for the Immobilized Low Activity Waste Performance Assessment (ILAW PA)*, PNNL-13037, Rev. 1, Pacific Northwest National Laboratory, Richland, Washington.
- Khaleel, R., and J.F. Relyea, 1997, "Correcting Laboratory-Measured Moisture Retention Data for Gravels," *Water Resources Research*, Vol. 33, pp. 1875-1878.
- Khaleel, R., J.F. Relyea, and J.L. Conca, 1995, "Evaluation of van Genuchten-Mualem Relationships to Estimate Unsaturated Conductivity at Low Water Contents," *Water Resources Research*, Vol. 31, pp. 2659-2668.
- Khaleel, R., T.-C.J. Yeh, and Z. Lu, 2002a, "Upscaled Flow and Transport Properties for Heterogeneous Unsaturated Media," *Water Resources Research*, Vol. 38(5), p. 1053, doi:10.1029/2000WR000072.
- Khaleel, R., T.-C.J. Yeh, Z. Lu, 2002b, "Effective Hydraulic Conductivity and Macrodispersivity Estimates for Heterogeneous Unsaturated Media," In *Computational Methods in Water Resources*, Proceedings of the XIV International Conference on Computational Methods in Water Resources, Delft, The Netherlands.
- Khaleel, R., T.E. Jones, A.J. Knepp, F.M. Mann, D.A. Myers, P.M. Rogers, R.J. Serne, and M.I. Wood, 2000, *Modeling Data Package for S-SX Field Investigation Report (FIR)*, RPP-6296, Rev. 0, CH2M HILL Hanford Group, Inc., Richland, Washington.
- Kincaid, C.T., J.W. Shade, G.A. Whyatt, M.G. Piepho, K. Rhoads, J.A. Voogd, J.H. Westsik, Jr., M.D. Freshley, K.A. Blanchard, and B.G. Lauzon, 1995, *Performance Assessment of Grouted Double-Shell Tank Waste Disposal at Hanford*, WHC-SD-WM-EE-004, Rev. 1, Westinghouse Hanford Company, Richland, Washington.
- Lee, T.A., 2004, *Single-Shell Tank System Closure Plan*, RPP-13774, Rev. 2, CH2M HILL Hanford Group, Inc., Richland, Washington.
- Millington, R.J., and J.P. Quirk, 1961, "Permeability of Porous Solids," *Trans. Faraday Soc.*, Vol. 57, pp. 1200-1207.
- Mualem, Y., 1976, "A New Model Predicting the Hydraulic Conductivity of Unsaturated Porous Media," *Water Resources Research*, Vol. 12, pp. 513-522.

Polmann, D.J., 1990, *Application of Stochastic Methods to Transient Flow and Transport in Heterogeneous Unsaturated Soils*, Ph.D. Thesis, Massachusetts Institute of Technology, Cambridge, Massachusetts.

*Resource Conservation and Recovery Act of 1976*, Public Law 94-580, 90 Stat. 2795, 42 USC 901 et seq.

Talbott, M.E., and L.W. Gelhar, 1994, *Performance Assessment of a Hypothetical Low-Level Waste Facility: Groundwater Flow and Transport Simulation*, NUREG/CR-6114, Vol. 3, U.S. Nuclear Regulatory Commission, Washington, D.C.

van Genuchten, M.Th., 1980, "A Closed-Form Solution for Predicting the Conductivity of Unsaturated Soils," *Soil Science Society of America Journal*, 44:892-898.

van Genuchten, M.Th., F.J. Leij, and S.R. Yates, 1991, *The RETC Code for Quantifying the Hydraulic Functions of Unsaturated Soils*, EPA/600/2-91/065, U.S. Environmental Protection Agency, Washington, D.C.

WAC 173-303, "Dangerous Waste Regulations," *Washington Administrative Code*, as amended.

Ward, A.L., G.W. Gee, and M.D. White, 1997, *A Comprehensive Analysis of Contaminant Transport in the Vadose Zone Beneath Tank SX-109*, PNNL-11463, Pacific Northwest National Laboratory, Richland, Washington.

Wing, N.R., 1994, *Permanent Isolation Surface Barrier Development Plan*, WHC-0673, Westinghouse Hanford Company, Richland, Washington.

Wood, M.I., T.E. Jones, B.N. Bjornstad, D.G. Horton, S.M. Narbutovskih, and R. Schalla, 2003, *Subsurface Conditions Description of the C and A-AX Waste Management Areas*, RPP-14430, Rev. 0, CH2M HILL Hanford Group, Inc., Richland, Washington.

Wurstner, S.K., P.D. Thorne, M.A. Chamness, M.D. Freshley, and M.D. Williams, 1995, *Development of a Three-Dimensional Ground-water Model of the Hanford Site Unconfined Aquifer System, FY 1995 Status Report*, PNL-10886, Pacific Northwest National Laboratory, Richland, Washington.

**APPENDIX A**  
**WASTE MANAGEMENT AREA C**  
**CLOSURE NUMERIC CALCULATIONS**

## CONTENTS

A1.0	INTRODUCTION .....	A-1
A2.0	REFERENCE ANALYSIS CASES .....	A-1
A3.0	SENSITIVITY AND “WHAT IF” CASES .....	A-2
	A3.1 RECHARGE.....	A-3
	A3.2 SOURCE TERM.....	A-9
	A3.3 HYDROLOGIC PARAMETERS.....	A-10
A4.0	THREE-DIMENSIONAL MODELING .....	A-11
A5.0	REFERENCES .....	A-12

## TABLES

A-1.	Summary of Reference Case Parameters and Expected Ranges .....	A-4
A-2.	Alternatives to the Reference Case or “What if” Conditions for the Examination of the Level of Protectiveness Provided by the Reference Case for the Protection of Groundwater .....	A-6

## TERMS

### Terms

bgs	below ground surface
$K_d$	distribution coefficient
MUST	miscellaneous underground storage tank
WMA	waste management area

### Units

%	percent
$\text{cm}^2/\text{s}$	square centimeters per second
ft	foot
m	meter
m/day	meters per day
mL/g	milliliters per gram
mm/yr	millimeters per year

## A1.0 INTRODUCTION

The source terms for the risk assessment consist of three separate sources that include: 1) past releases, 2) tank waste residuals, and 3) ancillary equipment residuals. The past releases include tank leaks and unplanned releases or spills; these represent contaminants which have leaked into the vadose zone and have migrated through the vadose zone for a number of years. Releases from the residual wastes (both from tank and tank ancillary equipment) in most cases would occur over a long period of time following closure of the tank farm when infiltrating water would enter the tank, dissolve contaminants, and migrate into the vadose zone and to the groundwater. The ancillary equipment residuals consist of residual wastes in pipelines and in miscellaneous underground storage tanks (MUST). The following items are common to the simulation runs to be performed:

- All calculations are for the row of tanks in C tank farm containing tanks 241-C-103, 241-C-106, 241-C-109, and 241-C-112.
- Unit inventories will be used for all sources.
- Following calculations for a unit inventory, contaminant breakthrough curves will be scaled for the actual inventory and a spatial and temporal superposition will be used to obtain breakthrough curves for the entire waste management area (WMA) based on results for a single tank.
- All calculations will be performed for 10,000 years following tank farm closure (i.e., from years 2032 to 12032).
- A two-dimensional vadose zone flow and transport model will be used for the integrated saturated-unsaturated flow domain up to the WMA fenceline.
- Streamtube models will be used to route contaminants from the WMA fenceline to the 200 Area exclusion boundary and to the Columbia River
- A series of mobile to moderately retarded contaminant species (distribution coefficient [ $K_d$ ] = 0, 0.02, 0.1, 0.2, 0.6, 1.0, 2.0, and 5.0 mL/g) will be considered.
- Recharge rate will be 100 mm/yr from years 2000 to 2032, 0.5 mm/yr from years 2032 to 2532, and 1.0 mm/yr thereafter.
- Isothermal assumption will be used.

## A2.0 REFERENCE ANALYSIS CASES

Table A-1 summarizes the reference analysis case parameters and the expected ranges in these parameters for the WMA C simulations. The features and processes associated with inventory do not require separate simulations because the resulting fluxes to groundwater are proportional to the assumed inventory. Separate simulations for  $K_d$  are covered by the range of values prescribed in the preceding section.

Flow and transport simulations will be run for the following reference analysis cases:

- **Case R1: Residual tank waste.** Residual tank waste source with a diffusion-dominated release rate (diffusion coefficient =  $1 \times 10^{-9}$  cm<sup>2</sup>/s), a release start date of January 1, 2032 and release over the tank bottom.

- **Case R2: Residual waste in pipelines.** Residual tank ancillary equipment waste source from pipelines with inventory located at a depth of 25 ft below ground surface (bgs), over an inventory diameter of 25 ft, situated between tanks 241-C-109 and 241-C-112, and a release start date of January 1, 2000.
- **Case R3: Residual MUST waste.** Residual MUST waste source with a diffusion dominated release rate (diffusion coefficient =  $1 \times 10^{-9}$  cm<sup>2</sup>/s), a release start date of January 1, 2032, and release over the tank bottom.
- **Case R4: Past tank leaks.** A past tank leak with its vadose zone inventory at a depth of about 150 ft (45.7 m) bgs and an inventory diameter of 25 ft (8 m) as of January 1, 2000, with the inventory distributed between tanks 241-C-109 and 241-C-112.
- **Case R5: Past spills.** An unplanned release with its vadose zone inventory at a depth of about 30 ft (9.2 m) bgs and an inventory diameter of 25 ft (8 m) as of January 1, 2000, with the inventory distributed between tanks 241-C-109 and 241- C-112.

Note:

1. For each tank, for each contaminant, and for each source term (i.e., residual waste, tank ancillary equipment waste, and past releases), the outputs based on tank 241-C-112 will be scaled.
2. Outputs will be at the WMA fenceline, 200 Area exclusion boundary, and the Columbia River (before mixing). The location of the boundaries will be based on streamtubes developed from the Hanford Site-wide groundwater model (Wurstner et al. 1995, *Development of a Three-Dimensional Ground-water Model of the Hanford Site Unconfined Aquifer System, FY 1995 Status Report*; Cole et al. 2001, *Transient Inverse Calibration of Hanford Site-Wide Groundwater Model to Hanford Operational Impacts - 1943 to 1996*).

### A3.0 SENSITIVITY AND “WHAT IF” CASES

A number of simulation cases have been identified to examine the functionality and capability of each feature of the natural and engineered barrier system to support the projected performance of the entire system. These simulation cases have been organized into cases that reflect the ranges in parameters important to contaminant release and transport to the groundwater (i.e., sensitivity or parameter range cases) and cases based on alternative conditions (i.e., “what if” cases) that reflect unexpected events, changes in the environmental conditions, undiscovered site characteristics, or unexpected (adverse) performance of the grouted waste.

Table A-1 presents the reference case parameters and expected ranges for various natural and engineered features. Table A-2 presents the “what if” cases or alternatives to the reference case for various natural and engineered features. Simulation cases have been identified that combine information presented in Tables A-1 and A-2; the simulation cases are grouped under Recharge (Section A.2.1), Source Term (Section A.2.2) and Hydrologic Parameters (Section A.2.3). Thus, the parameter ranges for the sensitivity (i.e., parameter range) cases are based on the ranges provided in Table A-1 and discussed further in Sections A.2.1 through A.2.3. Similarly, the alternate “what if” cases are provided in Table A-2 and discussed further in Sections A.2.1 through A.2.3.

Simulations will be performed for each waste source (i.e., past leaks, residual tank waste, and residual ancillary equipment waste). For each case, all other parameters in the simulation are the reference case values provided in Table A-1.

### A3.1 RECHARGE

Recharge sensitivity and “what if” cases examine the effects of changing parameters related to recharge on contaminant concentrations at the WMA fenceline. The following parameter effects are considered in the recharge analyses:

- Changes in the recharge rate during the tank farm operational period (1945 to 2032 for WMA C) (sensitivity analyses):
  - Reference case is 100 mm/yr
  - High case is 140 mm/yr (feature/process P1 maximum in Table A-1)
  - Low case is 40 mm/yr (feature/process P1 minimum in Table A-1)
- Recharge rate changes during and after the design life of the barrier (2032 to 2532) (sensitivity analyses):
  - Reference case is 0.5 mm/yr during the design life of the barrier
  - High case is 1.0 mm/yr during the design life of the barrier (feature/process P2 maximum in Table A-1)
  - Low case is 0.1 mm/yr during the design life of the barrier (feature/process P2 minimum in Table A-1)
  - Reference case is 1.0 mm/yr after the design life of the barrier
  - High case is 3.5 mm/yr after the design life of the barrier (feature/process P3 maximum in Table A-1)
  - Low case is 0.5 mm/yr after the design life of the barrier (feature/process P3 minimum in Table A-1)
  - Barrier failure in year 2332 (3.0 mm/yr at WMA C) (alternative A8 in Table A-2)
  - Barrier failure in year 2532 (3.0 mm/yr at WMA C) (alternative A7 in Table A-2)
  - Irrigated farming begins in year 2532 (50 mm/yr) (alternative A6 in Table A-2)
- Changes in recharge resulting from different emplacement times of the barrier (“what if” analyses):
  - Reference case is final barrier placed over WMAs in 2032
  - Interim barrier placement in 2010 over past leaks (alternative A3 in Table A-2)
  - Final barrier placed over WMAs in 2020 (alternative A1 in Table A-2)
  - Final barrier placed over WMAs in 2050 (alternative A2 in Table A-2).

**Table A-1. Summary of Reference Case Parameters and Expected Ranges (2 pages)**

Natural and Engineered Barriers/Features	Feature/Process	Reference Case	Parameter Range	
			Minimum	Maximum
Surface cover	P1: Recharge	A recharge rate of 100 mm/yr for the reference case during tank farm operation up to 2032.	40 mm/yr	140 mm/yr
	P2: Recharge	A recharge rate of 0.5 mm/yr for the reference case for the barrier from 2032 to 2532.	0.1 mm/yr	1.0 mm/yr
	P3: Recharge	A recharge rate of 1.0 mm/yr for the reference case for the barrier from 2532 to 12032	0.5 mm/yr	3.5 mm/yr
Grouted tank structure	P4: Residual release – diffusion coefficient	Diffusion-dominated release for residual tank wastes with a diffusion coefficient of $1 \times 10^{-9}$ cm <sup>2</sup> /sec for the reference case.	1.0 E-14 cm <sup>2</sup> /sec	1.0 E-08 cm <sup>2</sup> /sec
	P5: Waste residual – inventory	1 in. of waste	0.1 in. of waste residual	10 in. of waste residual
Vadose zone	P6: Past leaks depth – 200 East	150 ft bgs	130 ft bgs	170 ft bgs
	P7: Past Leaks Depth – 200 West <sup>b</sup>	130 ft bgs	110 ft bgs	150 ft bgs
	P8: Past Releases – inventory	Reference case inventory (Corbin et al. 2005)	Note <sup>a</sup>	Note <sup>a</sup>
	P9: Unsaturated flow	Variation of unsaturated hydraulic conductivity via saturated hydraulic conductivity, $K_{sat}$ (defined for each vadose zone layer)	$K_{sat} \times 0.1$ for each layer	$K_{sat} \times 10$ for each layer
	P10: Uranium $K_d$	Reference case uranium of 0.6 mL/g	0.2 mL/g	4 mL/g
	P11: Iodine $K_d$	Reference case iodine of 0.2 mL/g	0.1 mL/g	2 mL/g
	P12: Technetium $K_d$	Reference case technetium of 0.0 mL/g	0 mL/g	0.1 mL/g
Unconfined aquifer – 200 East Area WMAs	P14: Hydraulic conductivity	3,000 m/day	2,000 m/day	4,000 m/day
	Effective porosity	0.25	NC	NC
	Hydraulic gradient	0.00001	NC	NC
	Depth to water table	79 m (259 ft)	NC	NC
	Diffusion coefficient	$2.5 \times 10^{-5}$ cm <sup>2</sup> /sec	NC	NC

A-4

**Table A-1. Summary of Reference Case Parameters and Expected Ranges (2 pages)**

Natural and Engineered Barriers/Features	Feature/Process	Reference Case	Parameter Range	
			Minimum	Maximum
Unconfined aquifer – 200 West Area WMAs <sup>b</sup>	P15: Hydraulic conductivity	25 m/day	7.5 m/day	50 m/day
	Effective porosity	0.1	NC	NC
	Hydraulic gradient	0.0005	NC	NC
	Depth to water table	78m (256 ft)	NC	NC
	Diffusion coefficient	$2.5 \times 10^{-5} \text{ cm}^2/\text{sec}$	NC	NC
Unconfined aquifer – beyond 200 East and 200 West Area WMA fencelines <sup>b</sup>	Longitudinal macrodispersivity	62.5 m	NC	NC
	Lateral macrodispersivity	12.5 m	NC	NC
	Vertical macrodispersivity	0.0002 m	NC	NC

<sup>a</sup> The expected ranges (minimum and maximum) of release volume estimates will be based on Field and Jones (2005); the release volume estimates are in gallons. Inventories of radiological and nonradiological contaminants will be linearly scaled based on the contaminant concentration estimates provided for the reference case and listed in Corbin et al. (2005).

<sup>b</sup> Analyses for 200 West Area WMAs will be conducted under Khaleel et al. (2005).

NC = not considered

**Table A-2. Alternatives to the Reference Case or “What if” Conditions for the Examination of the Level of Protectiveness Provided by the Reference Case for the Protection of Groundwater (3 pages)**

<b>Barrier/Feature</b>	<b>Alternative</b>	<b>Condition</b>	<b>Description/Action</b>
Surface Barrier	A1	What is impact of closing the farm before 2032?	An earlier (2020) placement of the final closure interim barrier (as opposed to 2032 for the reference case)/sensitivity case.
	A2	What is the impact of not closing the farms by 2032?	A later (2050) placement of the final closure barrier will be examined/sensitivity case.
	A3	What is the impact of an interim barrier by 2010 over major leaks?	An interim barrier will be placed over the large leaks in WMAs S-SX and C beginning in the year 2010/sensitivity case.
	A4	What is the impact of episodic recharge?	Will not be analyzed. The impacts of episodic recharge are considered sufficiently analyzed in past work by Smoot et al. (1989). The results will be summarized, as appropriate.
	A5	What if the barrier subsides?	Will not be analyzed. Degradation of the effectiveness of the barrier due to localized subsidence. It is believed that any useful analysis of this issue at this time requires a more advanced closure and barrier design conceptualization.
	A6	What if irrigated farming occurs after the loss of passive control (500 years)?	Based on information in Mann et al. (2001), an enhanced recharge rate of 50 mm/yr is assumed to occur over the closed tank farm with the cover assumed removed. Enhanced recharge would begin at the end of passive institutional controls/sensitivity case.
	A7	What if the barrier fails at the end of passive controls?	Assume that the barrier fails at the end of passive controls (500 years). Failure is assumed through loss of silt-loam mix and recharge increases to background of 3.0 mm/yr in the 200 East Area and 4.0 mm/yr in the 200 West Area (Last et al. 2004)/sensitivity case.
	A8	What if the barrier fails prior to the end of passive controls?	Assume that the barrier fails at the end of 300 years. Failure is assumed through loss of silt-loam mix and recharge increases to background of 3.0 mm/yr in the 200 East Area and 4.0 mm/yr in the 200 West Area (Last et al. 2004)/sensitivity case.

**Table A-2. Alternatives to the Reference Case or “What if” Conditions for the Examination of the Level of Protectiveness Provided by the Reference Case for the Protection of Groundwater (3 pages)**

<b>Barrier/Feature</b>	<b>Alternative</b>	<b>Condition</b>	<b>Description/Action</b>
Grouted Tank/ Structure	A9a	What if the 100-Series tanks leak during retrieval?	9a: Simulate a retrieval leak loss of 8,000 gal per tank for a 100-Series tank that is assumed to be by the modified sluicing retrieval method/sensitivity case.
	A9b		9b: Simulate a retrieval leak loss of 20,000 gal per tank for a 100-Series tank that is assumed to be retrieved by the modified sluicing retrieval method/sensitivity case.
	A9c		9c: Simulate a retrieval leak loss of 8,000 gal per tank for a 100-Series tank, occurring over a past leak /sensitivity case.
	A10	What if retrieval leaks occur at the 200-Series tanks, regardless of the use of dry retrieval methods?	Simulate the effects of a 400-gal leak for each 200-Series tank/sensitivity case.
	A11	What if the grout does not provide the level of encapsulation expected?	Conduct a bounding analysis of this situation based on the assumption of an advection-dominated release for residual tank wastes/sensitivity case.
	A12	What if more tank waste residual is left than expected?	This possibility is addressed in the sensitivity analysis of possible ranges of tank residual waste (Table A-1).
	A13	What if a water line breaks over a past spill prior to tank stabilization?	Will not be analyzed. Report waterline leak effects for the reference case using conditions simulated in WMA S-SX field investigation report (Knepp 2002).
	A14	What if the tanks behave like a “bathtub” and collect water, which then releases suddenly?	Will not be analyzed. The void space left within the tank after grout fill is minimal. This is considered a highly unlikely scenario and is bounded by other analyses.
Vadose Zone	A15	What if potential preferential paths were missed during characterization?	Incorporate clastic dike effects for the retrieval leak simulation of 8,000 gal for a 100-Series tank that is assumed to be retrieved by the modified sluicing retrieval method /sensitivity case.
	A16	What if the groundwater level does not decline as projected?	Simulate the effect by decreasing the vadose zone thickness by 2 m/sensitivity case.
	A17	What if the depths of past leaks were underestimated?	This contingency is addressed in the sensitivity analysis (Table A-1).
	A18	What if past leak contamination were underestimated?	This contingency is addressed in the sensitivity analysis (Table A-1).
	A19	What if remediation of up to 50% of past leaks were possible?	Simulate the removal or immobilization of 5%, 25%, and 50% of mobile contaminants from past leaks/sensitivity case.
	A20	What is the effect of assuming anisotropy for the vadose zone geologic units?	Simulate assuming isotropic saturated hydraulic conductivity for the individual geologic units within the vadose zone /sensitivity case.

**Table A-2. Alternatives to the Reference Case or “What if” Conditions for the Examination of the Level of Protectiveness Provided by the Reference Case for the Protection of Groundwater (3 pages)**

<b>Barrier/Feature</b>	<b>Alternative</b>	<b>Condition</b>	<b>Description/Action</b>
Unconfined Aquifer	A21	What if the plume moves faster in the aquifer than predicted?	The high variability in the saturated hydraulic conductivity incorporates this potential variability (Table A-1).
	A22	What if the reference case assumption on groundwater flow is incorrect and more flow than expected flows north through Gable Gap?	Will not be analyzed for C tank farm. Such an impact will be investigated for T tank farm, assuming northerly flow through the Gable Gap.

### A3.2 SOURCE TERM

Contaminant source term sensitivity and “what if” analyses examine the effects of varying source term related parameters on contaminant concentrations at the WMA fenceline. The following source term related parameters are used in the contaminant inventory analyses:

- Changing the contaminant inventory of tank waste residuals (sensitivity case):
  - Reference case residuals remain 1 in. in height across tank bottom after retrieval
  - High case waste residuals remain 10 in. in height across tank bottom after retrieval (feature/process P5 maximum in Table A-1; also alternative A12 in Table A-2)
  - Low case waste residuals remain 0.1 in. in height across tank bottom after retrieval (feature/process P5 minimum in Table A-1)
- Changing the rate of diffusional release of tank waste residuals (sensitivity case):
  - Reference case diffusion coefficient for release of tank waste residuals is  $1.0 \times 10^{-9} \text{ cm}^2/\text{s}$
  - High case diffusion coefficient for release of tank waste residuals is  $1.0 \times 10^{-8} \text{ cm}^2/\text{s}$  (feature/process P4 maximum in Table A-1)
  - Low case diffusion coefficient for release of tank waste residuals is  $1.0 \times 10^{-14} \text{ cm}^2/\text{s}$  (feature/process P4 minimum in Table A-1)
- Using different tank waste residual release models (advection-dominated release compared to diffusion-dominated release) (“what if” case):
  - Reference case is diffusion-dominated release of tank waste residuals
  - Advection-dominated release of tank waste residuals (alternative A11 in Table A-2)
- Varying the volume (and hence contaminant inventory) of past release plumes (sensitivity case):
  - Reference case, high case, and low case past release volumes listed in Field and Jones (2005), *Tank Farm Vadose Zone Contamination: Volume Estimates* (feature/process P8 minimum and maximum in Table A-1; also alternative A18 in Table A-2)
- Varying the contaminant inventory of past release plumes (“what if” case):
  - Reference case contaminant inventory (Corbin et al. 2005, *Hanford Soil Inventory*)
  - Remove, treat, and dispose 50% of vadose zone contamination (alternative A19 in Table A-2)
  - Remove, treat, and dispose 25% of vadose zone contamination (alternative A19 in Table A-2)
  - Remove, treat, and dispose 5% of vadose zone contamination (alternative A19 in Table A-2)

- Considering the possibility of leakage during retrieval (“what if” case):
  - Reference case is negligible leakage during retrieval
  - Retrieval leak of 8,000 gal from 100-Series tanks (alternative A9a in Table A-2)
  - Retrieval leak of 20,000 gal from 100-Series tanks (alternative A9b in Table A-2)
  - Retrieval leak of 400 gal from 200-Series tanks (alternative A10 in Table A-2)
  - Retrieval leak of 8,000 gal from 100-Series tanks occurring over a past release (alternative A9c in Table A-2).

The retrieval leak is modeled as starting on January 1, 2000 and leaking at a uniform rate for 14 days, with the leak occurring at the bottom east corner of tank 241-C-112. A unit inventory is assumed to be readily available for transport with the infiltrating water where transport is only limited by chemical sorption with the sediments.

### A3.3 HYDROLOGIC PARAMETERS

Hydrologic parameter sensitivity and “what if” analyses examine the effects of variation in hydrologic parameters on contaminant concentrations at the WMA fenceline. The parameter changes used include:

- Changing contaminant  $K_d$  for tank waste residuals and past releases (sensitivity case):
  - Reference case contaminant  $K_d$  of technetium-99 is 0 mL/g
  - High case contaminant  $K_d$  of technetium-99 is 0.1 mL/g (feature/process P12 maximum in Table A-1)
  - Reference case contaminant  $K_d$  of iodine-129 is 0.2 mL/g
  - High case contaminant  $K_d$  of iodine-129 is 2 mL/g (feature/process P11 maximum in Table A-1)
  - Low case contaminant  $K_d$  of iodine-129 is 0.1 mL/g (feature/process P11 minimum in Table A-1)
  - Reference case contaminant  $K_d$  of uranium is 0.6 mL/g
  - High case contaminant  $K_d$  of uranium is 4 mL/g (feature/process P10 maximum in Table A-1)
  - Low case contaminant  $K_d$  of uranium is 0.2 mL/g (feature/process P10 minimum in Table A-1)
- Varying the depth of past release plumes (sensitivity case):
  - Reference case past release contaminant plume located 150 ft bgs at WMA C
  - High case past release contaminant plume located 130 ft bgs at WMA C (feature/process P6 minimum in Table A-1; also alternative A17 in Table A-2)
  - Low case past release contaminant plume located 170 ft bgs at WMA C (feature/process P6 maximum in Table A-1; also alternative A17 in Table A-2)

- Differences in the hydraulic conductivity of the vadose zone units (sensitivity analyses):
  - Reference case hydraulic conductivity of the vadose zone units
  - Higher case of unsaturated hydraulic conductivity of the vadose zone units in which the saturated hydraulic conductivity of individual units is increased by a factor of 10 (feature/process P9 maximum in Table A-1)
  - Lower case of unsaturated hydraulic conductivity of the vadose zone units in which the saturated hydraulic conductivity of individual units is decreased by a factor of 0.1 (feature/process P9 minimum in Table A-1)
- Changes in the unconfined aquifer hydraulic conductivity (sensitivity analyses):
  - Reference case hydraulic conductivity of the aquifer unit is 3,000 m/day at WMA C
  - Higher case of aquifer hydraulic conductivity with the reference value increased to 4,000 m/day at WMA C (feature/process P14 maximum in Table A-1; also alternative A21 in Table A-2)
  - Lower case of aquifer hydraulic conductivity with the reference value decreased to 2,000 m/day at WMA C (feature/process P14 minimum in Table A-1; also alternative A21 in Table A-2)
- Variation in the rate of water table decline (“what if” analyses):
  - Reference case water table elevation at WMA C is 79 m bgs
  - Water table elevation at WMA C is 77 m bgs (alternative A16 in Table A-2)
- The presence of clastic dikes (“what if” analyses):
  - Retrieval leak of 8,000 gal from 100-Series tanks occurring over a clastic dike (alternative A15 in Table A-2)
- The impact of not including anisotropic hydraulic conductivity parameters:
  - Reference case includes moisture dependent anisotropy function (Polmann model) to calculate vadose zone hydraulic conductivity for individual geologic units
  - Vadose zone hydraulic conductivity assumed to be isotropic (alternative A20 in Table A-2).

#### **A4.0 THREE-DIMENSIONAL MODELING**

A full three-dimensional flow and transport ( $K_d = 0$  mL/g) model for the C tank farm will be performed for a retrieval leak of 4,000 gallons at the bottom east corner of tank 241-C-112. The geologic cross-section for the C tank farm will form the basis for the three-dimensional model. The primary purpose of the three-dimensional analysis is to obtain a dilution factor so that the tank farm fenceline contaminant breakthrough curves on the basis of two-dimensional modeling results can be adjusted to account for the third dimension.

## A5.0 REFERENCES

- Cole, C.R., M.P. Bergeron, S.K. Wurstner, P.D. Thorne, S. Orr, and M.I. McKinley, 2001, *Transient Inverse Calibration of Hanford Site-Wide Groundwater Model to Hanford Operational Impacts - 1943 to 1996*, PNNL-13447, Pacific Northwest National Laboratory, Richland, Washington.
- Corbin, R.A., B.C. Simpson, M.J. Anderson, W.F. Danielson III, J.G. Field, T.E. Jones, M.D. Freshley, and C.T. Kincaid, 2005, *Hanford Soil Inventory Model, Rev. 1*, RPP 26744, Rev. 0, CH2M HILL Hanford Group, Inc., Richland, Washington.
- Field, J.G., and T.E. Jones, 2005, *Tank Farm Vadose Zone Contamination Volume Estimates*, RPP-23405, Rev. 1, CH2M HILL Hanford Group, Inc, Richland, Washington.
- Khaleel, R., M.P. Connelly, and W.J. McMahon, 2005, *Modeling Data Package for an Initial Assessment of Closure of the S and SX Tank Farms*, RPP-17209, Rev. 1, CH2M HILL Hanford Group, Inc., Richland, Washington.
- Knepp, A.J., 2002, *Field Investigation Report for Waste Management Area S-SX*, RPP-7884, Rev. 0, CH2M HILL Hanford Group, Inc., Richland, Washington.
- Last, G.V., W.E. Nichols, and C.T. Kincaid, 2004, *Geographic and Operational Site Parameters List (GOSPL) for the 2004 Composite Analysis*, PNNL-14725, Rev. 0, Pacific Northwest National Laboratory, Richland, Washington.
- Mann, F.M., K.C. Burgard, W.R. Root, R.J. Puigh, S.H. Finrock, R. Khaleel, D.H. Bacon, E.J. Freeman, B.P. McGrail, S.K. Wurstner, and P.E. LaMont, 2001, *Hanford Immobilized Low-Activity Waste Performance Assessment: 2001 Version*, DOE/ORP 2000 24, Rev. 0, U.S. Department of Energy, Office of River Protection, Richland, Washington.
- Smoot, J.L., J.E. Szecsody, B. Sagar, G.W. Gee, and C.T. Kincaid, 1989, *Simulations of Infiltration of Meteoric Water and Contaminant Plume Movement in the Vadose Zone at Single-Shell Tank 241-T-106 at the Hanford Site*, WHC-EP-0332, Westinghouse Hanford Company, Richland, Washington.
- Wurstner, S.K., P.D. Thorne, M.A. Chamness, M.D. Freshley, and M.D. Williams, 1995, *Development of a Three-Dimensional Ground-water Model of the Hanford Site Unconfined Aquifer System, FY 1995 Status Report*, PNL-10886, Pacific Northwest National Laboratory, Richland, Washington.

**APPENDIX B**  
**ADVECTION- AND DIFFUSION-DOMINATED RELEASE**  
**MODELS FOR RESIDUAL WASTES**

## CONTENTS

B1.0	INTRODUCTION .....	B-1
B2.0	CONCEPTUAL MODEL OF SOURCE TERM RELEASE .....	B-1
B3.0	MATHEMATICAL MODELS OF RELEASE MECHANISMS FOR THE ADVECTION- AND DIFFUSION-DOMINATED MODELS .....	B-2
B4.0	ADVECTION-DOMINATED RELEASE MODEL .....	B-2
B5.0	DIFFUSION DOMINATED RELEASE MODEL.....	B-3
B6.0	TANK ANCILLARY EQUIPMENT .....	B-5
B7.0	REFERENCES .....	B-6

## TERMS

### Units

%	percent
Ci/yr	curies per year
cm <sup>2</sup> /sec	square centimeter per second
ft	foot
ft <sup>3</sup>	cubic feet
in.	inch
KL	one thousand liters
L	liter
m	meter
m/yr	meters per year
yr	year

## **B1.0 INTRODUCTION**

The source terms for the risk assessment consist of three separate sources that include: 1) past releases, 2) tank waste residuals, and 3) tank ancillary equipment residuals. The past releases (i.e., past tank leaks and spills) represent tank wastes which have leaked into the vadose zone and have been migrating through the vadose zone for a number of years.

Releases from the tank waste residuals in most cases would occur over a long time period following closure of the tank farm when infiltrating water would enter the tank, dissolve contaminants, and release contaminants into the vadose zone and to the groundwater. For releases from tank waste residuals, an advection-dominated and a diffusion-dominated release model are considered (Wood et al. 1995, *Performance Assessment for the Disposal of Low-Level Waste in the 200 West Area Burial Grounds*). Release durations for these two models are not fixed a priori. A detailed description of the two models is presented later. First, the conceptual basis and assumptions for the source term release from tank waste residuals are presented.

## **B2.0 CONCEPTUAL MODEL OF SOURCE TERM RELEASE**

The actual process of contaminant (i.e., radionuclides and hazardous chemicals) release for residual tank wastes cannot be modeled precisely because of the variety of physical and chemical processes that occur between the waste material and the infiltrating water. In the real system, contaminants are distributed in a heterogeneous manner within the tank. These contaminants are released into solution at different rates because of the variability in waste material. Finally, variable types and quantities of contaminants are dissolved into the infiltrating water over time, depending on which waste material contacts a particular fluid volume. Therefore, averaging concepts are used in modeling to simplify the mathematical representation of the real system. These concepts must be justified, however, as being a conservative representation of the real system.

The following assumptions are made for the source-term release estimates:

- The release of contaminants from tank residuals is evaluated assuming that the structural integrity of the tanks degrades, allowing recharge (infiltrating) water to enter the tank, and dissolve contaminants from the residuals. The release of contaminants occurs by dissolution of the waste material contaminants into the infiltrating water migrating into and out of tanks through cracks.
- For stabilized (i.e., grouted) and degraded grouted wastes in the tank, it is assumed that the contaminant inventory will be available for release into the infiltrating moisture via a diffusion-dominated release model and an advection-dominated release model, respectively.
- Unit quantities are assumed for various modeling runs. Because contaminant transport calculations and risk estimates are directly proportional to total inventory, the modeling runs with unit quantities can be scaled to calculate risk for an estimated inventory.

- For those stabilized waste materials that are incorporated into a waste form that controls radionuclide release by diffusion (i.e., grouted waste), it is assumed that the diffusion coefficient remains constant over time for the diffusion-dominated release model.
- Tank residual wastes are assumed to be relatively insoluble and heterogeneously distributed within the tank.
- For the stabilized, grouted wastes, it is assumed that grouting will minimize direct moisture flow path, and the diffusional release from tank bottom is characterized by a mixing length, as described later.

### B3.0 MATHEMATICAL MODELS OF RELEASE MECHANISMS FOR THE ADVECTION- AND DIFFUSION-DOMINATED MODELS

The mathematical description and conditions under which the two different mechanisms occur are provided in the following sections. The area under each release scenario (i.e., advection- or diffusion-dominated release) is equal to the unit inventory.

#### B4.0 ADVECTION-DOMINATED RELEASE MODEL

The advection-dominated release model (mixing-cell cascade model) is used to simulate release from degraded grouted wastes. Such a waste type is represented by backfill material (i.e., sand and gravel), and the contaminants exit the facility at a rate determined by the flow of water and the amount of dispersion (mixing) within the tank. The mixing-cell cascade model (Kozak et al. 1990, *Background Information for the Development of a Low-Level Waste Performance Assessment Methodology*) is based on the dispersion analysis of chemical reactors and allows the analysis to incorporate the effects of dispersion within the tank in a simplified manner. In this model, the tank interior is considered to be composed of a cascade of  $N$  equal-sized, well-stirred cells in series. The total volume of  $N$  cells is equal to the volume of the tank residual waste within the mixing zone.

The mixing-cell cascade model for  $N$  equal-sized cells is described by the following equation:

$$Q(t) = qAC_0 \exp^{-\alpha Nt} \sum_{n=1}^N \frac{(\alpha Nt)^{n-1}}{(n-1)!} \quad \text{Equation B-1}$$

where:

$Q$  = release rate (Ci/yr)

$t$  = time (yr)

$q$  = vertical Darcy flux (m/yr)

$A$  = horizontal (planar) area of the tank interior

$C_0$  = initial concentration

$\alpha$  =  $q/(\theta dR)$

$\theta$  = volumetric moisture content in the residual waste

$d$  = vertical mixing depth (m)

$R$  = retardation factor in the waste material (assumed  $R = 1$ ).

The initial concentration of contaminant in the interstitial water can be determined from the following equation:

$$C_0 = \frac{m}{\theta VR} \quad \text{Equation B-2}$$

where:

$m$  = total facility inventory (assumed unity) of the radionuclides in the tank

$V$  = total volume of the residual waste (i.e., 360 ft<sup>3</sup> [10.2 kL] for 100-Series tanks and 30 ft<sup>3</sup> [850 L] for 200-Series tanks or 1% residual in accordance with *Hanford Federal Facility Agreement and Consent Order* [Ecology et al. 1989]).

The spatially variable velocities,  $V$ , and moisture contents,  $\theta$ , which are obtained via flow modeling within the tank, are used to determine  $C_0$ . For advection-dominated release, backfill is used as the tank fill material.

The mixing-cell cascade model provides results equivalent to that for one-dimensional, convective-dispersion equation with varying values of the dispersion coefficient (Kozak et al. 1990). In the limit, as  $N$  approaches infinity, the model represents flow through a system with zero dispersion, whereas for  $N$  equal to one, the model represents flow with an infinite dispersion coefficient. A value of  $N = 10$  will be used reflecting moderate dispersion.

## B5.0 DIFFUSION DOMINATED RELEASE MODEL

The diffusion-dominated release model is used to simulate the release of contaminants from stabilized (e.g., grouted tank) wastes. In the absence of little or no advection through the grouted waste, the release can be modeled as a diffusion-limited process. The diffusion from cylindrical containers leads to an expression for flux that contains infinite series (Kozak et al. 1990). The series converges slowly for small diffusion coefficients for short times, and even for relatively long times. As a result, a one-dimensional diffusion solution can be adopted (Crank 1975, *The Mathematics of Diffusion*). For a semi-infinite medium with the concentration  $C_0$  throughout, initially, and with zero surface concentration, the release of contaminants from the tank bottom, is given by:

$$C = C_0 \operatorname{erf} \frac{x}{2\sqrt{(D_e t)}} \quad \text{Equation B-3}$$

where:

$\operatorname{erf}$  = standard error function

$D_e$  = effective diffusion coefficient of the radionuclides in the waste form

$C$  = estimated concentration

$C_0$  = initial concentration

$t$  = time.

The rate of loss of diffusing substance per unit area from the semi-infinite medium, with the surface concentration being zero, is given by the following equation:

$$\left(D_e \frac{\partial C}{\partial x}\right)_{x=0} = C_0 \sqrt{\frac{D_e}{\pi t}} \quad \text{Equation B-4}$$

This equation has the form of diffusive mass transfer based on leaching theory.

The simplified release model leads to the following equation:

$$q = A C_0 \sqrt{\frac{D_e}{\pi t}} \quad \text{Equation B-5}$$

where:

$q$  = release rate from a single waste cell (Ci/yr)

$A$  = effective surface area of a single cell

$C_0$  = concentration in a cell.

The residual waste is likely contained in various cells with differing sizes and shapes. For the release model used herein, the cells were assumed to be of the same size and shape so that the diffusive release rate,  $Q$ , from all residual wastes in a tank can be based on the following equation:

$$Q = C_0 \sqrt{\frac{D_e}{\pi t}} \sum_{i=1}^n A_i$$

**Equation B-6**

$$= C_0 A_t \sqrt{\frac{D_e}{\pi t}}$$

where:

$n$  = number of cells

$A_i$  = surface area of individual cells

$A_t$  = total surface area.

Assuming that the cells are of constant size leads to the following equation:

$$I = C_0 \sum_{i=1}^n V_i = C_0 V_t \quad \text{Equation B-7}$$

where:

$I$  = total inventory

$V_i$  = volume of  $i$ -th cell

$V_t$  = total volume of all cells.

Combining the preceding equations leads to the following equation:

$$Q = I \frac{A_t}{V_t} \sqrt{\frac{D_e}{\pi t}} \quad \text{Equation B-8}$$

Equation B-8 is a reasonable approximation as long as the diffusional release time is much greater than the vadose zone travel time. The diffusion coefficient value for the reference analysis case is  $1 \times 10^{-9}$  cm<sup>2</sup>/sec

In Equation B-8, the surface area to volume ratio,  $A_t/V_t$ , can be interpreted as the mixing length for the diffusional release from the tank bottom. The mixing length value used in the diffusion-dominated release model, however, is much larger than the uniform thickness of the residual wastes in the tanks. The mixing length accounts for the heterogeneous distribution of residual wastes within a tank as well as the thick concrete structure for the diffusional release of contaminants from the tank. First, the residual wastes are not expected to be homogeneously distributed as a uniform thickness of 1 in. Following pouring of grout in the tank, the release from the tank occurs over a time period that exceeds thousands of years. During this long time period, contaminants within the residual wastes are transported by downward diffusion into the underlying concrete structure as well as by upward diffusion into “clean” grout.

For the concrete structure, Smith (2005), *Tank Farm Documented Safety Analysis*, states for the 100-Series tanks, “Each SST shell has an approximate 1-ft thick concrete base slab, dome and cylindrical wall that rests on a circular footing integral with the tank and base slab.”

The upward diffusive length ( $L$ ) is estimated to be about 18 in. Thus, for release calculations, the residual waste, prior to release, resides within the tank bottom thickness of 18 in. This, plus the “average” 12-in. thickness, plus other tank structural components, such as 2 in. of grout within the tank, 3/8 in. of mastic material (an asphalt liner), and 3/8-in. steel liner, accounts for the 0.825 m of mixing length ( $A_t/V_t$ ) used in the release model.

## B6.0 TANK ANCILLARY EQUIPMENT

Ancillary equipment is defined as structures, piping and equipment outside of the waste tanks but associated with tank farm operations. Evaluating ancillary equipment is an important component of the retrieval and closure strategy evaluation because the residual waste in tank ancillary equipments is a potential source term for either worker exposures (if the equipment was to be removed), or long-term risk (if the equipment was left in the tank farm). For the purpose of the risk assessment for WMA C, the ancillary equipment residuals consist of residual wastes in pipelines and in miscellaneous underground storage tanks. As described in Appendix A, Section A.1, it is assumed that the residual wastes in pipelines will be available instantaneously for transport with the infiltrating water. Also, as described in Appendix A, Section A.1, similar to release of tank residuals, the release of contaminants from residual wastes in miscellaneous underground storage tanks is modeled as a diffusional release.

**B7.0 REFERENCES**

- Crank, J., 1975, *The Mathematics of Diffusion*, Oxford University Press, Oxford, England.
- Ecology, EPA, and DOE, 1989, *Hanford Federal Facility Agreement and Consent Order*, as amended, Washington State Department of Ecology, U.S. Environmental Protection Agency, and U.S. Department of Energy, Olympia, Washington.
- Kozak, M.W., M.S.Y. Chu, P.A. Mattingly, J.D. Johnson, and J.T. McCord, 1990, *Background Information for the Development of a Low-Level Waste Performance Assessment Methodology*, NUREG/CR-5453 [SAND89-2509], Volume 5, U.S. Nuclear Regulatory Commission, Washington, D.C.
- Smith, R.D., 2005, *Tank Farms Documented Safety Analysis*, RPP-13033, Rev. 0, CH2M HILL Hanford Group, Inc., Richland, Washington.
- Wood, M.I., R. Khaleel, P.D. Rittmann, A.H. Lu, S.H. Finfrock, R.J. Serne, K.J. Cantrell, and T.H. DeLorenzo, 1995, *Performance Assessment for the Disposal of Low-Level Waste in the 200 West Area Burial Grounds*, WHC-EP-0645, Westinghouse Hanford Company, Richland, Washington.

**APPENDIX C**  
**GEOLOGIC CROSS-SECTION FOR C TANK FARM**

**CONTENTS**

C1.0 INTRODUCTION ..... C-1  
C2.0 REFERENCES ..... C-4

**FIGURE**

C-1. Northwest-Southeast Cross-Section through C Tank Farm..... C-3

**TERMS**

**Abbreviations and Acronyms**

WMA waste management area

**Units**

ft foot  
m meter

## C1.0 INTRODUCTION

Waste management area (WMA) C lies along the gently sloping, north flank of Cold Creek bar, a large compound flood bar formed during Pleistocene ice-age floods (DOE-GJO 1988, *Tank Summary Data Report for Tank A-103*; Wood et al. 2000, *Subsurface Conditions Description of the B-BX-BY Waste Management Area*) at an elevation of about 650 ft (198 m). The present thickness of the vadose zone measures about 250 ft (76 m) in the vicinity of WMA C (Narbutovskih and Horton 2001, *RCRA Groundwater Monitoring Plan for Single-Shell Tank Waste Management Area A-AX at the Hanford Site*; Horton and Narbutovskih 2001, *RCRA Groundwater Monitoring Plan for Single-Shell Tank Waste Management Area C at the Hanford Site*). The geohydrologic model of the area in the vicinity of WMA C is based on boreholes located within 1000 ft (300 m) of the WMA and contains an update of previous geologic descriptions given for these areas (Caggiano and Goodwin 1991, *Interim-Status Groundwater Monitoring Plan for the Single-Shell Tanks*; Williams et al. 2000, *Revised Hydrostratigraphy for the Suprabasalt Upper Aquifer System, 200 East Area, Hanford Site*; Narbutovskih and Horton 2001; Horton and Narbutovskih 2001). The geology specific to WMA C was first described by Price and Fecht (1976), *Geology of the 241-C Tank Farm*, followed by Caggiano and Goodwin (1991). Most recently, the WMA C geology was summarized by Lindsey (in Narbutovskih et al. 1996, *Feasibility of CPT-Deployed Vertical Electrode Array in Single-Shell Tank Farms*) and by Lindsey and Reynolds (in Jones et al. 1998, *A Summary and Evaluation of Hanford Site Subsurface Contamination*). A total of five stratigraphic units lie within WMA C. The stratigraphic units are represented on the northwest-southeast cross-section (Figure C-1) and are described as follows:

- **Backfill (material type 1, sandy gravel)**

Backfill materials consist of unstructured, poorly-sorted mixtures of gravel, sand, and silt removed during tank excavation, and then later used as fill around the tanks. Backfill materials extend to depths of 50 ft within the tank farms. Most or all of the recent deposit eolian sand and silt material found elsewhere across the Hanford Site has been removed and replaced with backfill in the immediate vicinity of the tank farm WMAs.

- **Hanford formation - upper gravelly sequence (H1 unit, material type 4, gravelly sand)**

Hanford formation H1 unit consists of predominantly loose coarse-grained gravel and sand deposits, with minor beds of sand to silty sand. Coarser beds may contain boulder-sized materials. Only a few weight percent or less calcium carbonate has been measured in this unit. The isopach map of the Hanford formation H1 unit suggests the unit thickens along a northwest-southeast trending trough. The maximum thickness (approximately 100 ft [30 m]) of the H1 unit underlies WMA A-AX, but the H1 unit is thinner in the immediate vicinity of the tanks in C tank farm because much of the Hanford formation H1 unit was removed and replaced with backfill during tank farm construction.

- **Hanford formation – sand sequence (H2 unit, material type 2, sand)**

Hanford formation H2 unit consists of predominantly fine- to coarse-grained sand with lenses of silty sand to slightly gravelly sand. Minor sandy gravel to gravelly sand beds occur sporadically. Consolidation ranges from loose to compact; cementation is very

minor or absent, and total calcium carbonate content is generally only a few weight percent or less. Silt lenses and thinly interbedded zones of silt and sand are common but not abundant in the Hanford formation H2 unit. These thin (<1ft [0.3 m]) fine-grained zones generally cannot be correlated among boreholes and are not reflected in the gross gamma-ray logs or moisture data. The Hanford formation sand sequence (H2 unit) underlies the entire area beneath WMA C. The H2 unit thickens to the south and west (Figure C-1).

- **Hanford formation - lower gravelly sequence (H3 unit, material type 3, gravelly sand)**

Hanford formation H3 unit consists of predominantly gravelly facies of clast supported, sandy, pebble to boulder gravel to matrix supported pebbly sand. The maximum calcium carbonate measured is approximately 2.5 weight percent. The exact thickness of the Hanford formation H3 unit beneath WMA C is uncertain.

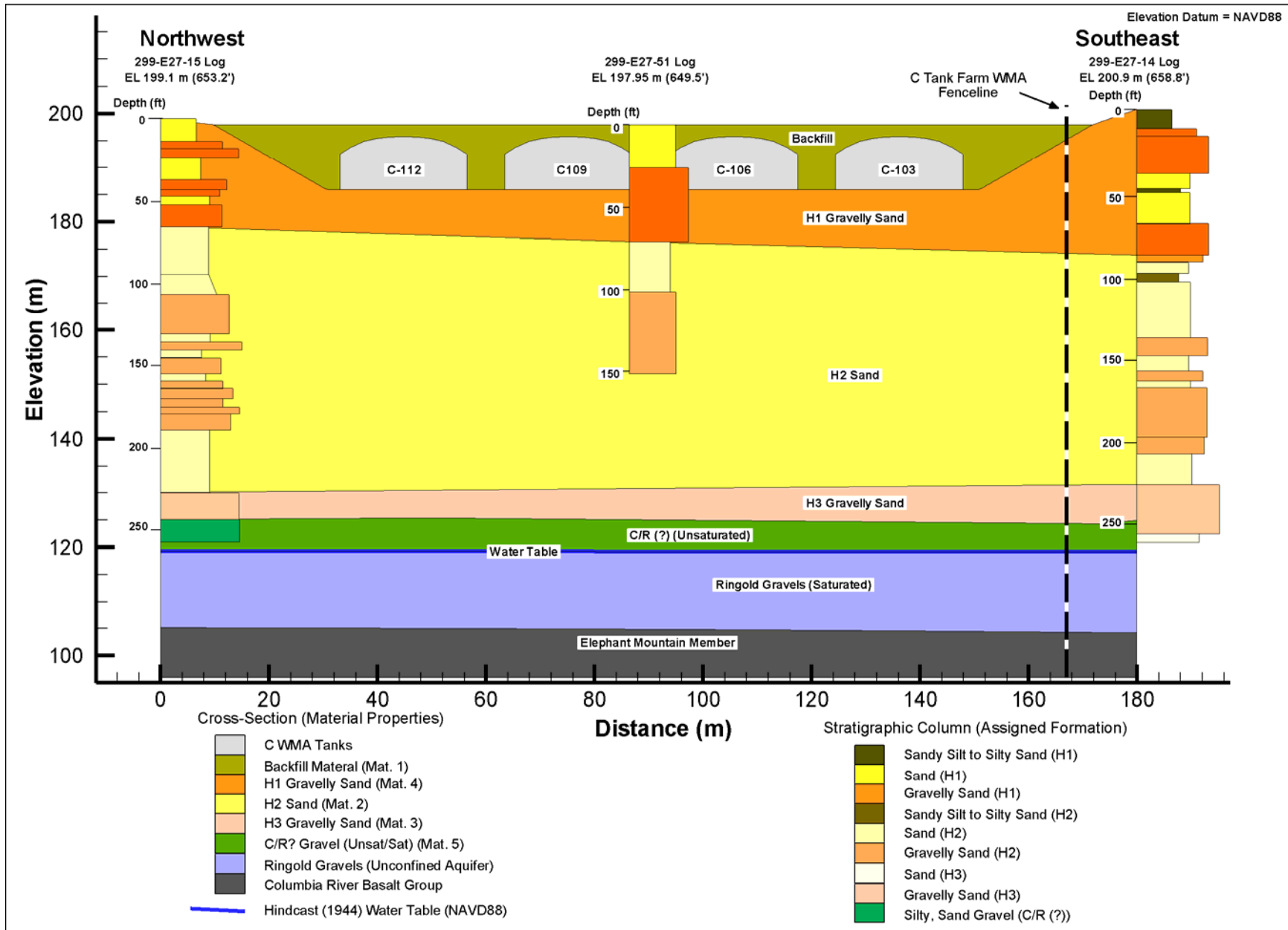
- **Undifferentiated Cold Creek Unit (pre-Missoula Gravels) and/or Ringold Formation UnitA? [material type 5]**

The Cold Creek Unit (pre-Missoula Gravels) and/or Ringold Formation UnitA? [material type 5] unit consists of predominantly sandy pebble- to cobble-sized gravel with occasional boulders. As a whole, the unit shares characteristics of both coarse-grained facies of the Ringold Formation and the Cold Creek Unit (pre-Missoula Gravels). In some boreholes, the unit is described as tight, cemented, and brown colored with oxide coatings (characteristics of the Ringold Formation), whereas borehole geologists' logs describe the unit as loose, caving to heaving, losing water, gray colored, and clean/unweathered (more characteristic of the Cold Creek Unit (pre-Missoula Gravels)). The total thickness of this unit is <90 ft (27 m), based on a limited number of boreholes where the upper and lower boundaries are represented. The top of Cold Creek Unit (pre-Missoula Gravels) and/or Ringold Formation UnitA? [material type 5] unit ranges between 341 to 407 ft (104 to 124 m) elevation above mean sea level. The water table lies within this unit.

- **Columbia River Basalt Group**

The Columbia River Basalt Group forms the bedrock base of the unconfined aquifer under WMA C. The top of the unit ranges from about 312 to 344 ft (95 to 105 m) elevation above mean sea level.

Figure C-1. Northwest-Southeast Cross-Section through C Tank Farm



C-3

## C2.0 REFERENCES

- Caggiano, J.A., and S.M. Goodwin, 1991, *Interim-Status Groundwater Monitoring Plan for the Single-Shell Tanks*, WHC-SD-EN-AP-012, Rev. 1, Westinghouse Hanford Company, Richland, Washington.
- DOE-GJO, 1998, *Tank Summary Data Report for Tank A-103*, GJ-HAN-108, U.S. Department of Energy, Grand Junction Office, Grand Junction, Colorado.
- Horton, D.G., and S.M. Narbutovskih, 2001, *RCRA Groundwater Monitoring Plan for Single-Shell Tank Waste Management Area C at the Hanford Site*, PNNL-13024, Pacific Northwest National Laboratory, Richland, Washington.
- Jones, T.E., R. Khaleel, D.A. Myers, J.W. Shade, and M.I. Wood, 1998, *A Summary and Evaluation of Hanford Site Subsurface Contamination*, HNF-2603, Rev. 0, Lockheed Martin Hanford, Richland, Washington.
- Narbutovskih, S.M., and D.G. Horton, 2001, *RCRA Groundwater Monitoring Plan for Single-Shell Tank Waste Management Area A-AX at the Hanford Site*, PNNL-13023, Pacific Northwest National Laboratory, Richland, Washington.
- Narbutovskih, S.M., D.F. Iwatate, M.D. Sweeney, A.L. Ramirez, W. Daily, R.M. Morey, and L. Christensen, 1996, *Feasibility of CPT-Deployed Vertical Electrode Array in Single-Shell Tank Farms*, WHC-SD-EN-TA-004, Rev. 0, Westinghouse Hanford Company, Richland, Washington.
- Price, W.H., and K.R. Fecht, 1976, *Geology of the 241-C Tank Farm*, ARH-LD-132, Atlantic Richfield Hanford Company, Richland, Washington.
- Williams, B.A., B.N. Bjornstad, R. Schalla, and W.D. Webber, 2000, *Revised Hydrogeology for the Suprabasalt Upper Aquifer System, 200 East Area and Vicinity, Hanford Site, Washington*, PNNL-12261, Pacific Northwest National Laboratory, Richland, Washington.
- Wood, M.I., R. Schalla, B.N. Bjornstad, and S.M. Narbutovskih, 2000, *Subsurface Conditions Description of the B-BX-BY Waste Management Area*, HNF-5507, Rev. 0, CH2M HILL Hanford Group, Inc, Richland, Washington.

**APPENDIX D**  
**WASTE MANAGEMENT AREA C VADOSE ZONE FLOW AND**  
**TRANSPORT PARAMETER ESTIMATES**

## CONTENTS

D1.0	SOIL HYDRAULIC PROPERTIES .....	D-1
D2.0	EFFECTIVE (UPSCALED) FLOW AND TRANSPORT PROPERTIES .....	D-4
D2.1	EFFECTIVE (UPSCALED) FLOW PARAMETERS .....	D-4
	D2.1.1 Stochastic Upscaling .....	D-4
D2.2	EFFECTIVE TRANSPORT PARAMETERS.....	D-10
	D2.2.1 Bulk Density and $K_d$ .....	D-11
	D2.2.2 Diffusivity.....	D-11
	D2.2.3 Dispersivity.....	D-11
D3.0	REFERENCES .....	D-21

## FIGURES

D-1.	Experimental (Triangles) and Fitted Theoretical (Squares) Variogram for LnKs.....	D-8
D-2.	Calculated Macroscopic Anisotropy (Equation D-3) as a Function of Mean Pressure Head for the Backfill (1) and Cold Creek (pre-Missoula gravels)/Ringold Sandy Gravel (5) Units .....	D-9
D-3.	Calculated Macroscopic Anisotropy (Equation D-3) as a Function of Mean Pressure Head for the Sandy H2 (2) Unit .....	D-9
D-4.	Calculated Macroscopic Anisotropy (Equation D-3) as a Function of Mean Pressure Head for the Gravelly Sand H3 (3) Sequence .....	D-10
D-5.	Calculated Macroscopic Anisotropy (Equation D-3) as a Function of Mean Pressure Head for the Gravelly Sand H1 (4) Unit .....	D-10
D-6.	Longitudinal Macrodispersivity in Saturated Media as a Function of Overall Problem Scale with Data Classified by Reliability (after Gelhar et al. 1992) .....	D-13
D-7.	Longitudinal Macrodispersivity in Unsaturated Media as a Function of Overall Problem Scale (after Gelhar 1993) .....	D-15
D-8.	Uranium LnK versus R for (a) Backfill (1) and Cold Creek (pre-Missoula gravels)/Ringold Sandy Gravel (5), (b) Sandy H2 (2), (c) Gravelly Sand H3 (3), and (d) Gravelly Sand H1 (4) at the C Tank Farm .....	D-19

## TABLES

D-1.	van Genuchten Parameters, Fitted Saturated Hydraulic Conductivity, and Measured Bulk Density Data for the Backfill (1) and Cold Creek (pre-Missoula gravels)/ Ringold Sandy Gravel (5) Sediments .....	D-2
D-2.	van Genuchten Parameters, Fitted Saturated Hydraulic Conductivity, and Measured Bulk Density Data for the Sandy H2 (2) Sequence.....	D-2
D-3.	van Genuchten Parameters, Fitted Saturated Hydraulic Conductivity, and Measured Bulk Density Data for the Gravelly Sand H3 (3) Sequence.....	D-3
D-4.	van Genuchten Parameters, Fitted Saturated Hydraulic Conductivity, and Measured Bulk Density Data for the Gravelly Sand H1 (4) Sediments .....	D-3
D-5.	Composite van Genuchten-Mualem Parameters for Various Strata at the C Tank Farm .....	D-6
D-6.	Macroscopic Anisotropy Parameters for Various Strata at the C Tank Farm .....	D-8
D-7.	Effective Parameter Estimates, $E[\rho_b K_d]$ , for Uranium for the Product of Bulk Density and $K_d$ at C Tank Farm.....	D-11
D-8.	Non-Reactive Macrodispersivity Estimates for Soils at the C Tank Farm.....	D-17
D-9.	Macrodispersivity Enhancement Estimates for Various Strata at the C Tank Farm [ $\rho_b$ in $\text{g}/\text{cm}^3$ and $K_d$ in $\text{cm}^3/\text{g}$ ].....	D-18

## TERMS

### Abbreviations and Acronyms

ERDF	Environmental Restoration Disposal Facility
$K_d$	distribution coefficient
PUREX	Plutonium-Uranium Extraction Facility
RETC	RETention Curve code

### Units

cm	centimeter
cm/s	centimeter per second
cm <sup>2</sup> /s	square centimeter per second
cm <sup>2</sup> /yr	square centimeter per year
cm <sup>3</sup> /cm <sup>3</sup>	cubic centimeter per cubic centimeter
cm <sup>3</sup> /g	cubic centimeter per gram
g/cm <sup>3</sup>	gram per cubic centimeter
L	liter
m	meter
mm	millimeter

## D1.0 SOIL HYDRAULIC PROPERTIES

No site-specific data on soil moisture characteristics are available for vadose zone sediments in the C tank farm. However, as part of other Hanford Site projects, particle-size distribution, saturated hydraulic conductivity, moisture retention, and unsaturated conductivity data have been collected in the vicinity of waste management area C. These sites include the Environmental Restoration Disposal Facility (ERDF), 241-T-106 tank site, and Operable Units 200-UP-1 and 200-UP-2 in the 200 West Area. Also available are physical and hydraulic properties data for the sandy gravel sediments in the 100 Area along the Columbia River. These samples were used as surrogates to represent the hydraulic properties for the gravel-dominated (>2 mm size fraction) sequence at the C tank farm.

Standard laboratory and Westinghouse Hanford Company quality assurance procedures (WHC 1991, *Geotechnical Engineering Procedure Manual*) were used to analyze the sediment samples. The moisture retention data for the fine fraction (< 2 mm) and for the drainage cycle of up to -1,000 cm of pressure head were measured using “Tempe” pressure cells; the rest of the drainage data up to -15,000 cm was measured using the pressure plate extraction method (Klute 1986, “Water Retention: Laboratory Methods”). Saturated hydraulic conductivities for the bulk samples (including gravels) were measured in the laboratory using constant-head permeameter. A variation of the unit gradient method (Klute and Dirksen 1986, “Hydraulic Conductivity and Diffusivity: Laboratory Methods”; Khaleel et al. 1995, “Evaluation of van Genuchten-Mualem Relationships to Estimate Unsaturated Conductivity at Low Water Contents”) was used to measure unsaturated hydraulic conductivities for the bulk samples. The laboratory measured data on < 2mm size fraction were corrected for the gravel fraction (Gardner 1986, “Water Content”; Khaleel and Relyea 1997, “Correcting Laboratory-Measured Moisture Retention Data for Gravels”). No correction was needed for the saturated and unsaturated conductivities, since these were measured on the bulk sample.

It is well recognized that the estimated unsaturated conductivities, based on saturated conductivity and the van Genuchten retention model, can differ by up to several orders of magnitude with measured conductivities at the dry end (e.g., Khaleel et al. 1995). Therefore, a simultaneous fit of both laboratory-measured moisture retention and unsaturated conductivity data was used in this work, and all five unknown parameters,  $\theta_r$ ,  $\theta_s$ ,  $\alpha$ ,  $n$ , and  $K_s$ , with  $m=1-1/n$  (van Genuchten 1980, “A Closed-Form Solution for Predicting the Conductivity of Unsaturated Soils”), were fitted to the data via a code named RETention Curve (RETC) (van Genuchten et al. 1991, *The RETC Code for Quantifying the Hydraulic Functions of Unsaturated Soils*). The pore size distribution factor,  $\ell$  (Mualem 1976, “A New Model for Predicting the Hydraulic Conductivity of Unsaturated Porous Media”) was kept fixed at 0.5 during the simultaneous fitting. The fitted parameters, based on moisture retention and unsaturated conductivity measurements for various strata are shown in Tables D-1 through D-4. Note that the numbers 1 through 5 in Tables D-1 through D-4 (and elsewhere) represent different strata at the C tank farm.

**Table D-1. van Genuchten Parameters, Fitted Saturated Hydraulic Conductivity, and Measured Bulk Density Data for the Backfill (1) and Cold Creek (pre-Missoula gravels)/Ringold Sandy Gravel (5) Sediments**

Sample	Site/ Operable Unit	Borehole Number	Depth m	Percent Gravel	$\theta_s$ cm <sup>3</sup> /cm <sup>3</sup>	$\theta_r$ cm <sup>3</sup> /cm <sup>3</sup>	$\alpha$ 1/cm	$n$	Fitted $K_s$ cm/s	Bulk Density g/cm <sup>3</sup>
4-0792	ERDF	699-35-65A	75.4	71	0.100	0.0084	0.03	1.5858	3.42E-04	2.32
4-1012	ERDF	699-35-69A	73.9	55	0.147	0	0.0076	1.5109	4.50E-05	2.19
4-1013	ERDF	699-35-69A	77.9	65	0.139	0.0127	0.0065	1.5656	1.06E-06	2.20
4-1079	ERDF	699-35-61A	90.9	61	0.163	0	0.014	1.3079	1.18E-04	2.06
4-1080	ERDF	699-35-61A	93.5	43	0.178	0	0.0074	1.3819	8.11E-06	2.00
3-0668	241-T-106	299-W10-196	38.9	62	0.175	0	0.0192	1.6124	1.63E-04	2.13
3-0682	241-T-106	299-W10-196	46.1	51	0.224	0	0.0166	1.6577	2.37E-04	2.14
3-0688	241-T-106	299-W10-196	48.5	49	0.199	0	0.0043	1.5321	2.60E-05	2.17
3-0689	241-T-106	299-W10-196	52.2	28	0.236	0	0.0025	1.4747	4.58E-05	1.93
3-0690	241-T-106	299-W10-196	53.7	53	0.1819	0.0177	0.0046	1.541	4.19E-05	2.19

**Table D-2. van Genuchten Parameters, Fitted Saturated Hydraulic Conductivity, and Measured Bulk Density Data for the Sandy H2 (2) Sequence**

Sample	Site/ Operable Unit	Borehole Number	Depth m	Percent Gravel	$\theta_s$ cm <sup>3</sup> /cm <sup>3</sup>	$\theta_r$ cm <sup>3</sup> /cm <sup>3</sup>	$\alpha$ 1/cm	$n$	Fitted $K_s$ cm/s	Bulk Density g/cm <sup>3</sup>
3-0589	241-T-106	299-W10-196	25.5	1	0.429	0.0268	0.0057	1.7173	4.73E-05	1.86
3-1707	200-UP-2	299-W19-95	9.5	15	0.364	0.0742	0.0082	2.0349	1.55E-05	1.86
3-1712	200-UP-2	299-W19-95	43.1	0	0.290	0.0362	0.0156	2.021	2.05E-04	1.71
3-1713	200-UP-2	299-W19-95	46.3	0	0.5026	0	0.0077	1.6087	2.51E-05	1.72
3-1714	200-UP-2	299-W19-95	50.8	2	0.394	0.1301	0.0061	1.535	1.05E-04	1.68
4-0637	ERDF	699-36-63A	74.9	0	0.378	0	0.0153	1.7309	6.89E-05	1.62
4-0642	ERDF	699-35-69A	25.7	0	0.353	0.0286	0.014	1.4821	6.81E-04	1.98
4-0644	ERDF	699-35-69A	49.8	0	0.394	0.0557	0.0076	1.8353	3.24E-05	1.89
4-0791	ERDF	699-35-65A	63.2	0	0.338	0.0256	0.0226	2.2565	6.81E-04	1.60
4-1076	ERDF	699-35-61A	76.4	0	0.357	0	0.0293	1.7015	1.23E-03	1.74
4-1111	200-UP-1	699-38-68A	56.9	1	0.394	0.0497	0.0093	1.4342	5.80E-05	1.69
4-1112	200-UP-1	699-38-68A	66.0	0	0.4346	0	0.0054	1.4985	2.49E-05	1.73

**Table D-3. van Genuchten Parameters, Fitted Saturated Hydraulic Conductivity, and Measured Bulk Density Data for the Gravelly Sand H3 (3) Sequence**

Sample	Site/ Operable Unit	Borehole Number	Depth m	Percent Gravel	$\theta_s$ cm <sup>3</sup> /cm <sup>3</sup>	$\theta_r$ cm <sup>3</sup> /cm <sup>3</sup>	$\alpha$ 1/cm	$n$	Fitted K <sub>s</sub> cm/s	Bulk Density g/cm <sup>3</sup>
3-0572-2	100-FR-3	199-F5-48	8.1	27	0.179	0	0.0031	1.4306	2.38E-05	2.03
3-0576	100-FR-3	199-F5-43B	5.4	20	0.244	0.0166	0.0167	1.5428	3.96E-04	1.95
3-1707	200-UP-2	299-W19-95	9.5	15	0.364	0.0742	0.0082	2.0349	1.55E-05	1.86
5-0149	218-E-12B	299-E34-1	24.4	16	0.260	0	0.0082	1.4422	1.80E-04	2.07
5-0150	218-E-12B	299-E34-1	24.84	17	0.240	0.0227	0.0295	1.7077	1.47E-03	1.95
5-0151	218-E-12B	299-E34-1	21.49	17	0.275	0	0.0049	1.4621	6.85E-05	1.95
5-0152	218-E-12B	299-E34-1	65.5	26	0.280	0.0252	0.0438	1.3253	2.43E-03	1.85
5-0157	218-E-10	299-E32-4	3.50	13	0.293	0.033	0.0273	2.1675	7.77E-03	1.88

**Table D-4. van Genuchten Parameters, Fitted Saturated Hydraulic Conductivity, and Measured Bulk Density Data for the Gravelly Sand H1 (4) Sediments**

Sample	Site/ Operable Unit	Well Number	Depth m	Percent Gravel	$\theta_s$ cm <sup>3</sup> /cm <sup>3</sup>	$\theta_r$ cm <sup>3</sup> /cm <sup>3</sup>	$\alpha$ 1/cm	$n$	Fitted K <sub>s</sub> cm/s	Bulk Density g/cm <sup>3</sup>
3-0210	241-T-106	299-W10-196	3.1	48	0.186	0.029	0.014	1.7674	1.96E-04	2.11
3-0572-2	100-FR-3	199-F5-48	8.1	27	0.179	0	0.0031	1.4306	2.38E-05	2.03
3-0576	100-FR-3	199-F5-43B	5.4	20	0.244	0.0166	0.0167	1.5428	3.96E-04	1.95
3-0668	241-T-106	299-W10-196	38.9	62	0.175	0	0.0192	1.6124	1.63E-04	2.13
3-0682	241-T-106	299-W10-196	46.1	51	0.224	0	0.0166	1.6577	2.37E-04	2.14
3-0688	241-T-106	299-W10-196	48.5	49	0.199	0	0.0043	1.5321	2.60E-05	2.17
3-0689	241-T-106	299-W10-196	52.2	28	0.236	0	0.0025	1.4747	4.58E-05	1.93
3-0690	241-T-106	299-W10-196	53.7	53	0.1819	0.0177	0.0046	1.541	4.19E-05	2.19
5-0152	218-E-12B	299-E34-1	65.5	26	0.280	0.0252	0.0438	1.3253	2.43E-03	1.85
5-0153	218-E-10	299-E32-4	10.7	47	0.214	0.0092	0.0099	1.3829	1.41E-04	2.08
5-0158	218-E-10	299-E32-4	71.6	44	0.217	0	0.0104	1.3369	4.47E-04	2.15

## **D2.0 EFFECTIVE (UPSCALED) FLOW AND TRANSPORT PROPERTIES**

Data on hydraulic properties, described in the preceding section, were obtained via laboratory tests on core samples (scales of the order of a few cm). However, numerical models of fluid flow and contaminant transport in the unsaturated zone require specifying hydraulic properties for each discretized grid block (scales of the order of meters). Therefore, the scale of the grid blocks is usually much larger than the scale at which the unsaturated properties were measured. The process of defining large-scale properties for the numerical grid blocks based on small, measurement-scale point measurements is called upscaling.

This section provides effective (upscaled) values of flow and transport parameters for the vadose zone. Specific flow parameters include moisture retention, and saturated and unsaturated hydraulic conductivity. Transport parameters include bulk density, diffusivity, sorption coefficients, and macrodispersivity.

### **D2.1 EFFECTIVE (UPSCALED) FLOW PARAMETERS**

Any attempt at upscaling is confronted with the issue of spatial variability of hydraulic properties due to small-scale soil heterogeneities. The presence of spatial variability in hydraulic properties of Hanford Site soils has been well documented (e.g., Khaleel and Freeman 1995, *Variability and Scaling of Hydraulic Properties for 200 Area Soils, Hanford Site*). A fundamental issue is then how best to incorporate the effects of natural heterogeneity in modeling. A traditional approach is to use deterministic models and attempt to incorporate the overall heterogeneity of the system such as layering while neglecting the small-scale heterogeneity. The considerable spatial variability of Hanford Site soils makes complete characterization of the hydraulic properties at the field scale an almost impossible task, as an enormous amount of data is required for proper representation of the actual media heterogeneities.

An alternative approach is to define an equivalent homogeneous medium with average, effective (upscaled) hydraulic properties that are related to the local small-scale heterogeneities and thereby predict the mean flow and transport behavior of the field-scale, larger media. However, to represent a heterogeneous medium by its homogeneous equivalent, we need to estimate the effective hydraulic properties that represent this equivalent homogeneous medium.

A straightforward approach would be to use statistical averages (arithmetic or geometric) of the local soil hydraulic properties, but such simple estimates may not always be able to properly describe the complicated nonlinear behavior in heterogeneous soils.

#### **D2.1.1 Stochastic Upscaling**

For saturated media, an averaging of the heterogeneities in geologic media at a smaller scale leads to an effective hydraulic conductivity value, at the larger (macroscopic) scale, with the lateral hydraulic conductivity being much larger than the vertical conductivity (Freeze and Cherry 1979, *Groundwater*). For unsaturated media, theoretical (e.g., Mualem 1984, "Anisotropy of unsaturated soils"; Yeh et al. 1985a, "Stochastic Analysis of Unsaturated Flow in Heterogeneous Soils, 1, Statistically Isotropic Media"; Yeh et al. 1985b, "Stochastic Analysis of Unsaturated Flow in Heterogeneous Soils, 2, Statistically Anisotropic Media with Variable  $\alpha$ "; Yeh et al. 1985c, "Stochastic Analysis of Unsaturated Flow in Heterogeneous Media, 3, Observations and Applications"; Bear et al. 1987, "Effective and Relative Permeabilities of

Anisotropic Porous Media”; Mantoglou and Gelhar 1987, “Stochastic Modeling of Large-Scale Transient Unsaturated Flow”; Green and Freyberg 1995, “State-Dependent Anisotropy: Comparisons of Quasi Analytical Solutions with Stochastic Results for Steady Gravity Drainage”) and experimental analyses (e.g., Stephens and Heerman 1988, “Dependence of Anisotropy on Saturation in a Stratified Sand”; Yeh and Harvey 1990, “Effective Unsaturated Hydraulic Conductivity of Layered Sands”; McCord et al. 1991, “Hysteresis and State Dependent Anisotropy in Modeling Unsaturated Hillslope Hydrologic Processes”) of field-scale unsaturated flow indicates that, in stratified sediments, the effective hydraulic conductivity tensor is anisotropic with a tension-dependent (or moisture-dependent) degree of anisotropy. The anisotropy ratio of horizontal hydraulic conductivity to vertical hydraulic conductivity increases with decreasing moisture content. Variable, moisture-dependent anisotropy in unsaturated soils is therefore an effective, large-scale (macroscopic) flow property which results from media heterogeneities at a smaller scale, and provides a framework for upscaling laboratory-scale measurements to the effective (upscaled) properties for the large-scale vadose zone.

#### **D2.1.1.1 Field Observations**

Field observations in the 200 Areas do indeed provide evidence of saturation-dependent anisotropy and lateral migration. A test facility comprising an injection well at the center and a radial array of 32 monitoring wells was constructed in 1980 south of the Plutonium-Uranium Extraction Facility (PUREX) in the 200 East Area. The facility was used in late 1980 and early 1981 to conduct an infiltration and multiple tracer (i.e., chloride, nitrate, barium, rubidium, strontium-85, and cesium-134) test, in which 45,000 L of liquid (in 11 increments) were injected at a depth of 4.7 m over a period of 133 days (Sisson and Lu 1984, *Field Calibration of Computer Models for Application to Buried Liquid Discharges: A Status Report*).

Three-dimensional water content profiles in layered, coarse sediments were monitored to a depth of 18 m by downhole neutron probe measurements. The initial water contents were measured at 30-cm increments over the 30- to 1800-cm depths in all 32 observation wells. In situ gamma energy analysis data were collected to determine the distribution of radioactive tracers. The unique three-dimensional nature of the experiment and the measured water content profiles provide evidence of tension-dependent anisotropy. The field data clearly show lateral spreading that occurred during injection. The horizontal wetting patterns dominated the experiment. In fact, numerical modeling results (Sisson and Lu 1984), based on the assumption of a uniform and isotropic model, show a much deeper penetration of the moisture profile than occurring in the field (Sisson and Lu 1984). The degree of spreading was remarkable considering the apparent uniform lithology at the site.

#### **D2.1.1.2 Composite Macroscopic Relationships**

Both moisture retention and unsaturated conductivity data show spatial variability, although the degree of variation at a given tension is more modest for moisture retention than for hydraulic conductivity. Based on data in Tables D 1 through D-4, composite parameters for the moisture retention relations were determined. The composite van Genuchten parameters for various strata were obtained via RETC (van Genuchten et al. 1991) and a simultaneous fit of both moisture retention and unsaturated conductivity predictions; all four unknown parameters,  $\theta_r$ ,  $\theta_s$ ,  $\alpha$ , and  $n$  with  $m=1-1/n$  (van Genuchten 1980), were fitted to the data. The pore size distribution factor  $\ell$

was kept constant at 0.5 during the simultaneous fitting. The saturated conductivity,  $K_s$ , was fitted to the data.

Table D-5 shows the fitted parameters. Equivalent horizontal and vertical hydraulic conductivities are derived using macroscopic anisotropy relations, as described in the next section.

**Table D-5. Composite van Genuchten-Mualem Parameters for Various Strata at the C Tank Farm**

Strata/Material Type	Number of Samples	$\theta_s$	$\theta_r$	$\alpha$ 1/cm	n	$\ell$	Fitted $K_s$ cm/s
Backfill (1)	10	0.1380	0.0100	0.0210	1.374	0.5	5.60E-04
Sand H2 (2)	12	0.3819	0.0443	0.0117	1.6162	0.5	9.88E-05
Gravelly Sand H3 (3)	8	0.2688	0.0151	0.0197	1.4194	0.5	5.15E-04
Gravelly Sand H1 (4)	11	0.2126	0.0032	0.0141	1.3730	0.5	2.62E-04
Cold Creek (pre Missoula gravels)/Ringold Sandy Gravel (5)	10	0.1380	0.0100	0.0210	1.374	0.5	5.60E-04

### D2.1.1.3 Stochastic Model for Macroscopic Anisotropy

Variable, tension-dependent anisotropy provides a framework for upscaling small-scale measurements to the effective (upscaled) properties for the large-scale vadose zone. A stochastic model is used to evaluate tension-dependent anisotropy for sediments at the C tank farm.

Yeh et al. (1985a, 1985b) analyzed steady unsaturated flow through heterogeneous porous media using a stochastic model; parameters such as hydraulic conductivity are treated as random variables rather than as deterministic quantities. The Gardner (1958), “Some Steady-State Solutions of the Unsaturated Moisture Flow Equation with Applications to Evaporation from a Water Table,” relationship was used by Yeh et al. (1985a, 1985b) to describe unsaturated hydraulic conductivity ( $K$ ) as a function of saturated hydraulic conductivity ( $K_s$ ) and tension ( $h$ ), i.e.,

$$K(h) = K_s \exp(-\beta h) \quad \text{Equation D-1}$$

where:

$\beta$  = fitting parameter.

Equation D-1 can be written as:

$$\ln K(h) = \ln K_s - \beta h \quad \text{Equation D-2}$$

Equation D-2 is referred to as the log-linear model, since  $\ln K$  is linearly related to  $h$  through the constant slope  $\beta$ . However, such a constant slope is often inadequate in describing  $\ln K(h)$  over ranges of tension of practical interest for field applications. As an alternative, the slope  $\beta$  can be approximated locally by straight lines over a fixed range of tension. The “ $\ln K_s$ ” term in Equation D-2 can then be derived by extrapolating the local slopes back to zero tension.

Using a linear correlation model between the log-conductivity zero-tension intercept and  $\beta$ , Polmann (1990), *Application of Stochastic Methods to Transient Flow and Transport in Heterogeneous Unsaturated Soils*, presents a generalized model that accounts for the cross correlation of the local soil property (i.e.,  $\ln K_s$  and  $\beta$ ) residual fluctuations. Compared to uncorrelated  $\ln K_s$  and  $\beta$  model, a partial correlation of the properties is shown to have a significant impact on the magnitude of the effective parameters derived from the stochastic theory. The Polmann (1990) equations for deriving the effective parameters are as follows.

$$\begin{aligned} \langle \ln K \rangle &= \langle \ln K_s \rangle - A \langle h \rangle - \sigma_{\ln K_s}^2 \lambda [p - p^2 \langle h \rangle - \zeta^2 \langle h \rangle] / (1 + A\lambda) \\ \sigma_{\ln K}^2 &= \sigma_{\ln K_s}^2 [(1 - p \langle h \rangle)^2 + \zeta^2 \langle h \rangle^2] / (1 + A\lambda) \\ K_h^{eq} &= \exp[\langle \ln K \rangle + (\sigma_{\ln K}^2 / 2)] \\ K_v^{eq} &= \exp[\langle \ln K \rangle - (\sigma_{\ln K}^2 / 2)] \end{aligned} \quad \text{Equation D-3}$$

where:

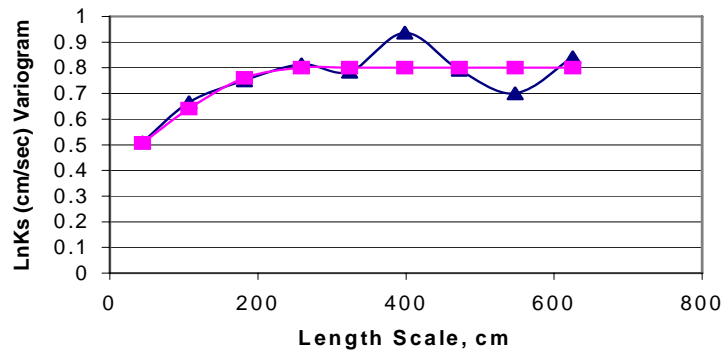
- $\sigma_{\ln K}^2$  = variance of log unsaturated conductivity (which depends on mean tension)
- $\langle h \rangle$  = mean tension
- $\sigma_{\ln K_s}^2$  = variance of  $\ln K_s$
- $\langle \ln K_s \rangle$  = mean of  $\ln K_s$
- $p$  = slope of the  $\beta$  versus  $\ln K_s$  regression line
- $\zeta$  =  $\sigma\delta / \sigma_{\ln K_s}$
- $\sigma\delta$  = standard deviation of the residuals in the  $\beta$  versus  $\ln K_s$  regression
- $A$  = mean slope,  $\beta$ , for  $\ln K_s$  vs.  $h$
- $\lambda$  = vertical correlation lengths for  $\ln K_s$  (assumed to be same as that of  $\beta$ )
- $K_h^{eq}$  = equivalent unsaturated horizontal conductivity
- $K_v^{eq}$  = equivalent unsaturated vertical conductivity.

#### D2.1.1.4 Macroscopic Anisotropy Relations

Results of application of Equation D-3 for variable anisotropy are presented below. The data for individual stratum (Tables D-1 through D 4) were used to obtain parameters  $\langle \ln K_s \rangle$ ,  $\sigma_{\ln K_s}^2$ ,  $p$ ,  $\zeta$ , and  $A$ . The slope and pseudo  $\ln K_s$  estimates, discussed in the preceding section, were evaluated for the moisture regime of interest (i.e., tension range of 500 cm to 700 cm for the sandy sequence and 700 cm to 1000 cm for the gravelly sequence). It should be noted, however, that no experimental data are available for unsaturated conductivities in the tension range of interest;  $\beta$  and  $\ln K_s$  estimates were based on the fitted van Genuchten-Mualem curves.

An estimate of the correlation length,  $\lambda$ , is needed for anisotropy calculations. Most of the measurements in the 200 Areas have been obtained at sampling intervals that are too coarse to yield a reasonable estimate for the correlation length. However, one data set is available that provides saturated conductivity estimates at about 30-cm intervals for a depth of 18 m within the Hanford formation; the site is located about 1/2 mile east of the Integrated Disposal Facility site in the 200 East Area. Figure D-1 shows the experimental variogram and the fitted spherical variogram model for saturated conductivities. The fitted spherical variogram suggests a correlation length,  $\lambda$ , of about 50 cm (i.e., the distance at which the variogram drops to  $[1 - (1/e)]$  times the sill [Figure D-1]). The correlation length,  $\lambda$ , for both  $\ln K_s$  and  $\beta$  were assumed to be equal.

**Figure D-1. Experimental (Triangles) and Fitted Theoretical (Squares) Variogram for LnKs**



The Polmann parameters for various strata are shown in Table D-6. Because of different  $A$ ,  $\langle \ln K_s \rangle$ ,  $\sigma_{\ln K_s}^2$ , and  $\zeta$  values, macroscopic anisotropy relations for the sandy and gravelly sediments are quite different. Figures D-2 through D-5 illustrate the macroscopic anisotropy relations for the four sediments, and will be used to assign anisotropy ratios for various strata. In general, the anisotropy for the gravelly soils is much less compared to that for sandy soils. Note that, for gravelly soils, no data were available for a variogram analysis. However, a smaller  $\lambda$  value (30 cm) is used (Table D-6) because of a much higher variance of  $\ln K_s$  for the gravelly soils than for the sandy soils.

**Table D-6. Macroscopic Anisotropy Parameters for Various Strata at the C Tank Farm**

Strata/Material Type	Number of Samples	$\theta_s$	$\theta_r$	$\alpha$ 1/cm	n	$\ell$	Fitted $K_s$ cm/s
Backfill (1)	10	0.1380	0.0100	0.0210	1.374	0.5	5.60E-04
Sand H2 (2)	12	0.3819	0.0443	0.0117	1.6162	0.5	9.88E-05
Gravelly Sand H3 (3)	8	0.2688	0.0151	0.0197	1.4194	0.5	5.15E-04
Gravelly Sand H1 (4)	11	0.2126	0.0032	0.0141	1.3730	0.5	2.62E-04
Cold Creek (pre-Missoula gravels)/Ringold Sandy Gravel (5)	10	0.1380	0.0100	0.0210	1.374	0.5	5.60E-04

**Figure D-2. Calculated Macroscopic Anisotropy (Equation D-3) as a Function of Mean Pressure Head for the Backfill (1) and Cold Creek (pre-Missoula gravels)/Ringold Sandy Gravel (5) Units**

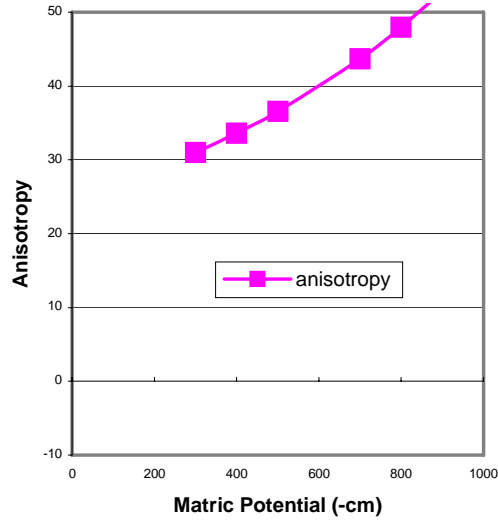


**Figure D-3. Calculated Macroscopic Anisotropy (Equation D-3) as a Function of Mean Pressure Head for the Sandy H2 (2) Unit**

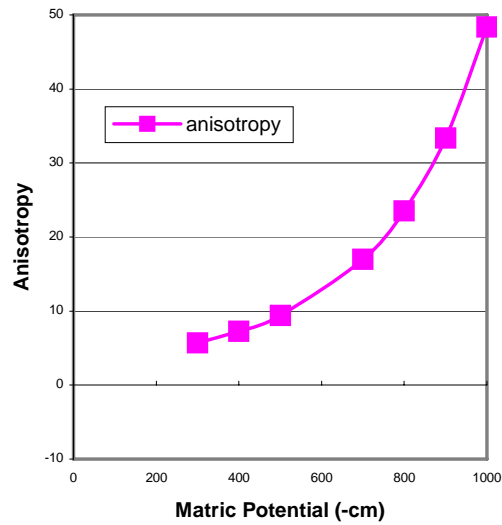


**Figure D-4. Calculated Macroscopic Anisotropy (Equation D-3) as a Function of Mean Pressure Head for the Gravelly Sand H3 (3) Sequence**

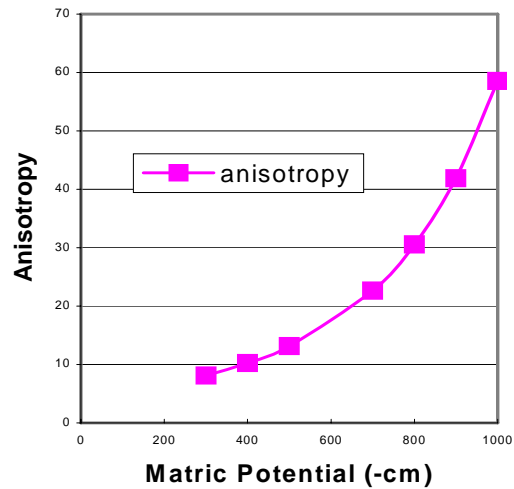
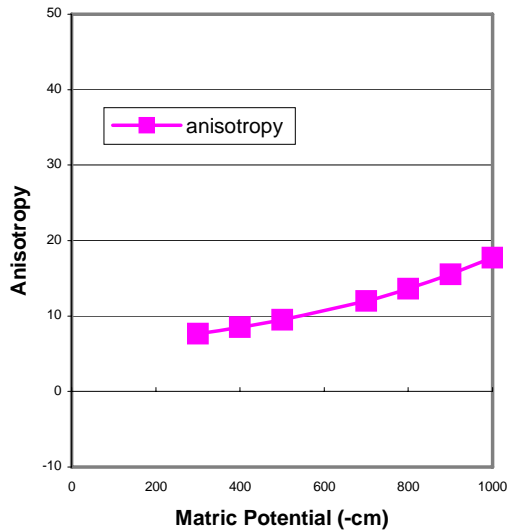


**Figure D-5. Calculated Macroscopic Anisotropy (Equation D-3) as a Function of Mean Pressure Head for the Gravelly Sand H1 (4) Unit**



## D2.2 EFFECTIVE TRANSPORT PARAMETERS

Base case effective transport parameter (i.e., bulk density, diffusivity, dispersivity) estimates are presented in this section. Because of natural variability, the transport parameters are all spatially variable. The purpose is again similar to the flow parameters, to evaluate the effect of such variability on the large-scale transport process.

### D2.2.1 Bulk Density and $K_d$

Both bulk density ( $\rho_b$ ) and distribution coefficient ( $K_d$ ) estimates are needed to calculate retardation factors for different species. The effective, large-scale estimate for the product  $[\rho_b K_d]$  is the average of the product of small-scale laboratory measurements for bulk density and  $K_d$  (Gelhar 1993, *Stochastic Subsurface Hydrology*). Table D-7 provides the effective, large-scale estimates for uranium. The average  $\rho_b$ ,  $E[\rho_b]$  (Table D-7) estimates are based on data in Tables D-1 through D-4 for various strata. The  $K_d$  estimates (Table D-7) for uranium are based on data for undisturbed sediments from Kaplan and Serne (2000), *Geochemical Data Package for the Immobilized Low-Activity Waste Performance Assessment*.

**Table D-7. Effective Parameter Estimates,  $E[\rho_b K_d]$ , for Uranium for the Product of Bulk Density and  $K_d$  at C Tank Farm**

Strata/Material Type	$K_d$ cm <sup>3</sup> /g	$E[\rho_b]$ g/cm <sup>3</sup>	$E[\rho_b K_d]$
Backfill (1) and Cold Creek (pre-Missoula gravels)/ Ringold Gravels (5)	0.6	2.13	0.59
Sandy H2 (2)	0.6	1.76	1.04
Gravelly sand H3 (3)	0.6	1.94	1.17
Gravelly sand H1 (4)	0.6	2.07	1.24

### D2.2.2 Diffusivity

It is assumed that the effective, large-scale diffusion coefficients for all strata at the C tank farm are a function of volumetric moisture content,  $\theta$ , and can be expressed using the Millington-Quirk (1961), "Permeability of Porous Solids," empirical relation:

$$D_e(\theta) = D_0 \frac{\theta^{10/3}}{\theta_s^2} \quad \text{Equation D-4}$$

where:

$D_e(\theta)$  = effective diffusion coefficient of an ionic species as a function of moisture content

$D_0$  = molecular diffusion coefficient for the same species in free water.

The molecular diffusion coefficient for all species in free water is assumed to be  $2.5 \times 10^{-5}$  cm<sup>2</sup>/sec (Kincaid et al.1995, *Performance Assessment of Grouted Double-Shell Tank Waste Disposal at Hanford*).

### D2.2.3 Dispersivity

An extended review is provided on the rationale of choice for vadose zone dispersivity estimates. Readers who are familiar with the state-of-the-art can proceed directly to Section D.2.2.3.4.

A variety of factors such as the size of the flow domain, the flow regime (saturated versus unsaturated flow), field heterogeneities, and the contaminant species (retarded versus non-retarded) need to be recognized in estimating dispersivities. The objective of this section is to provide appropriate guidance on the choice of vadose zone dispersivity estimates for use in transport modeling.

It should be noted that laboratory data would be of little use in estimating field-scale dispersivities. While well-designed, large-scale tracer experiments would provide useful information, limited field data are available at this time. Therefore, the dispersivity estimates needed for modeling are essentially based on literature values and the available stochastic equations.

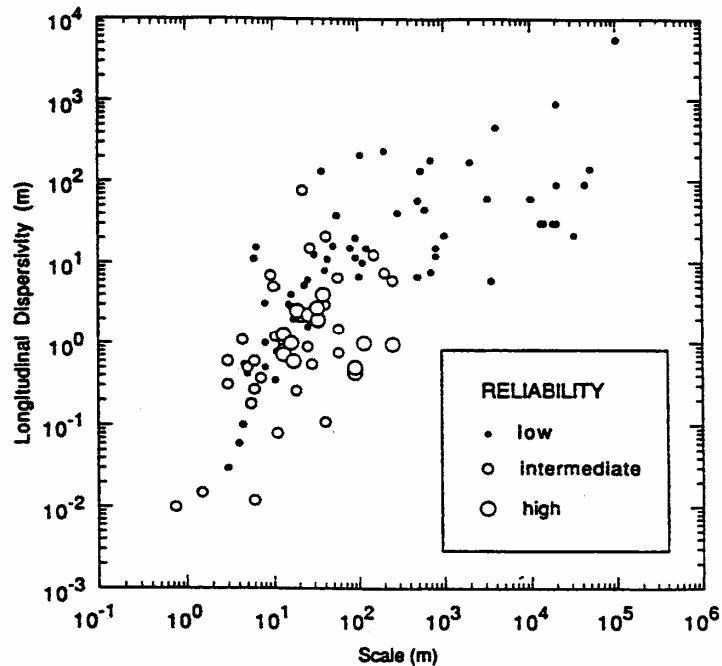
Literature data suggest that much more information is available on dispersion in saturated media than in unsaturated media. Therefore, first, the available data on dispersivities in saturated media are summarized (Gelhar et al. 1992, "A Critical Review of Data on Field-Scale Dispersion in Aquifers"). Second, available data on vadose zone dispersivities are presented, including results of small-scale tracer experiments in the 200 East Area. Third, the stochastic framework used in obtaining dispersivity estimates is reviewed, and estimates are provided for use in modeling.

#### **D2.2.3.1 Saturated Media Dispersivities for Field Sites**

A critical review of dispersivity observations from 59 different field sites was performed by Gelhar et al. (1992). Extensive tabulations of information were included by Gelhar et al. (1992) on aquifer type, hydraulic properties, flow configuration, type of monitoring network, tracer, method of data interpretation, overall scale of observation, and longitudinal, horizontal transverse, and vertical transverse dispersivities from original sources. The information was then used to classify the dispersivity data into three reliability classes, low, intermediate, and high. Overall, the data indicate a trend of systematic increase of the longitudinal dispersivity with observation scale but the trend is much less apparent when the reliability of data is considered (Figure D-6).

The longitudinal dispersivity ranged from  $10^{-1}$  to  $10^5$  m, but the largest scale for high reliability data was only 250 m. When the data are classified according to porous versus fractured media, no significant differences were apparent between these aquifer types. At a given scale, the longitudinal dispersivity values were found to range over 2 to 3 orders of magnitude and the higher reliability data approached the lower portion of this range. The high reliability dispersivity data ranged from a low of about 0.6 m at a scale of 15 m to about 1 m at a scale of 250 m; some data are on the order of 2 to 3.5 m at a scale of 30 m (Figure D-6).

**Figure D-6. Longitudinal Macrodispersivity in Saturated Media as a Function of Overall Problem Scale with Data Classified by Reliability (after Gelhar et al. 1992)**



It is not appropriate to represent the longitudinal dispersivity data by a single universal line. The variations in dispersivity reflect the influence of differing degrees of aquifer heterogeneity at different sites. The data on transverse dispersivities are more limited but clearly indicate that vertical transverse dispersivities are typically an order of magnitude smaller than horizontal transverse dispersivities (Gelhar et al. 1992). Re-analysis of data from several of the field sites showed that improved interpretations most often lead to smaller dispersivities (Gelhar et al. 1992).

Overall, Gelhar et al. (1992) concluded that longitudinal dispersivities in the lower part of the indicated range are more likely to be realistic for field situations. This suggests that, for conservative species, a longitudinal dispersivity on the order of a meter is a reasonable estimate for saturated media domains that are a couple of hundred meters in scale. Note that the estimates are for saturated media and conservative species. As discussed later, dispersivity estimates are enhanced due to heterogeneous sorption in both saturated and unsaturated media.

### **D2.2.3.2 Vadose Zone Dispersivities**

As discussed earlier for a tank farm with a surface barrier, the vadose zone water contents beneath the facility are expected to approach the natural moisture regime for arid soils. Although exceptional precipitation events may cause transient high water contents near the soil surface, the recharge is not likely to be sustained at great depths within the vadose zone.

This inference is supported by the results of artificial tracer experiments on much shorter time scales. For example, two massively instrumented solute transport experiments were performed

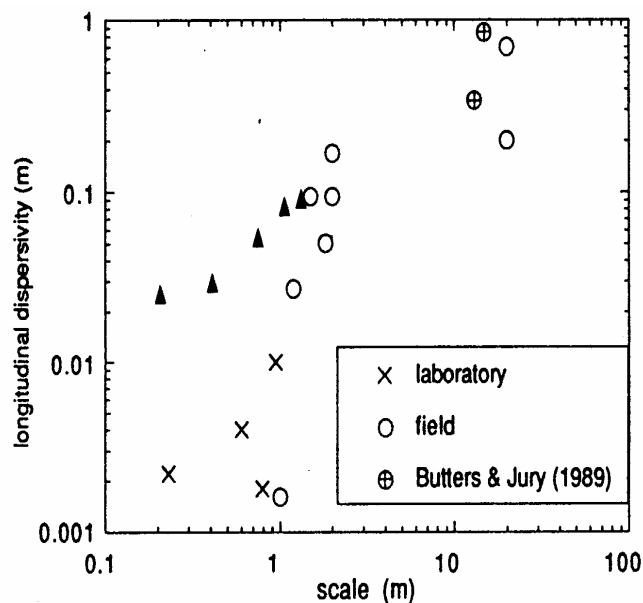
in desert soils near Las Cruces, New Mexico (Wierenga et al. 1991, “The Las Cruces Trench Site: Characterization, Experimental Results, and One-Dimensional Flow Predictions”; Hills et al. 1991, “The Second Las Cruces Trench Experiment: Experimental Results and Two-Dimensional Flow Predictions”). Drip emitters were used to irrigate a plot adjoining a deep trench in a heterogeneous soil possessing with more than one order of magnitude standard deviation in saturated hydraulic conductivity. Monitoring of the trench face showed a spatially uniform progression of the wetting front and did not reveal indications of preferential flow (Wierenga et al. 1991). Hills et al. (1991) found that a dispersivity of 5 cm provided reasonably realistic simulations of tritium and bromine tracer distributions.

For unsaturated flow, long-term environmental tracer studies at several arid southwestern sites indicate dispersivities of less than 10 cm. Phillips et al. (1988), “Chlorine-36 and Tritium from Nuclear-Weapons Fallout as Tracers for Long-Term Liquid and Vapor Movement in Desert Soils,” assessed the degree of mixing in desert soils using the conventional advection-dispersion modeling, yielding a dispersion coefficient of  $50 \text{ cm}^2/\text{yr}$ . This compares with the calculated effective diffusion coefficient of  $25 \text{ cm}^2/\text{yr}$ . A similar study by Scanlon (1992), “Evaluation of Liquid and Vapor Water Flow in Desert Soils Based on Chlorine 36 and Tritium Tracers and Nonisothermal Flow Simulations,” at another southwestern arid site, obtained a dispersion coefficient of about  $14 \text{ cm}^2/\text{yr}$ . These, then, lead to effective dispersivities of about 7 and 4 cm, at the two arid sites, and Peclet numbers (displacement divided by dispersivity) of 23 and 17.

Ward et al. (1998), *Determination of In Situ Hydraulic Parameters of the Upper Hanford Formation*, obtained dispersivity estimates via field measurements at a location in the 200 East Area, using potassium chloride as a tracer. Analysis of the data provided dispersivities that ranged from 1.3 to 7.8 cm for travel distances ranging from 25 to 125 cm. Dispersivity increased with depth to about 0.75 m, after which it essentially became constant. Although these estimates are for the Hanford formation, the transport distance within the vadose zone is indeed of limited extent. Nevertheless, results based on the limited data are consistent with the concept of a scale dependent dispersivity. Thus, although no data exist on large-scale dispersivities, it is expected that they will be larger than those based on the small-scale tracer experiment of Ward et al. (1998).

Based on a survey of literature, Gelhar (1993) presented the longitudinal vadose zone dispersivities as a function of the scale of the experiment (Figure D-7). Figure D-7 shows a lack of data for scales larger than 2 m. Nevertheless, similar to saturated flow, Figure D-7 shows an increase of dispersivity with an increase in scale. Also, shown in Figure D-7 are results from the Ward et al. (1998) experiment; their data are in close agreement with others.

**Figure D-7. Longitudinal Macrodispersivity in Unsaturated Media as a Function of Overall Problem Scale (after Gelhar 1993)**



*The triangles are data from Ward et al. 1998.*

### D2.2.3.3 Stochastic Models and Macrodispersivities for Large-Scale Media

Field-scale dispersivities are referred to as macrodispersivities. The heterogeneities that exist at various length scales result in a scale dependence of macrodispersivities. Stochastic models have been developed which relate the macrodispersive spreading to the spatial variability of saturated hydraulic conductivity field in a saturated porous media (e.g., Gelhar and Axness 1983, “Three Dimensional Analysis of Macrodispersion in a Stratified Aquifer”; Dagan 1984, “Solute Transport in Heterogeneous Porous Formations”). The Gelhar and Axness (1983) model provides the asymptotic estimates of macrodispersivity, while the Dagan (1984) model describes the preasymptotic estimates of macrodispersivities for the near-source, early time period. The Dagan (1984) model predicts that under steady state flow with a uniform mean hydraulic gradient, the ensemble longitudinal macrodispersivity increases with time and displacement distance as the solute first enters the flow domain. A constant, asymptotic value (i.e., Fickian behavior) is eventually reached after the solute travels a few tens of correlation scales of the hydraulic conductivity field.

For prediction of contaminant transport during early time or for short travel distances, simulating effects of scale-dependence on macrodispersion is a consideration. The dispersivities increase with time (or equivalently with distance) until they tend to converge on their unique asymptotic (large time) values. The second-moment evolution curve or the time-dependent, preasymptotic macrodispersivities are of particular interest, since it can take a long time (e.g., years or decades) for the asymptotic Fickian approximation to take hold. However, the early time scale dependencies are of little consequence in simulations involving long times or large mean travel distances such as those for C modeling. For these predictions over large travel distances or large times, the use of a constant (asymptotic) dispersivity is considered to be adequate. An estimate

of the maximum or asymptotic value of macrodispersivity for saturated media can be based on the Gelhar and Axness (1983) stochastic solution:

$$A_L = \sigma_{LnKs}^2 \lambda \quad \text{Equation D-5}$$

where:

$\lambda$  = vertical correlation scale (i.e., average distance over which conductivities are correlated) for log saturated hydraulic conductivity.

In addition to the size of flow domain and vadose zone soil heterogeneities, dispersivities are expected to be a function of soil moisture content (or matric potential). Macrodispersivities are expected to increase with a decrease in saturation (e.g., Polmann 1990). Russo (1993), “Stochastic Modeling of Macrodispersion for Solute Transport in a Heterogeneous Unsaturated Porous Formation,” suggests that vadose zone macrodispersivities can be defined in a manner similar to saturated media estimates. This is based on his finding that the product of the variance and the correlation scale of log conductivity for both saturated and unsaturated media are of similar magnitude. In other words, an increase in the variance of log conductivity (and concurrently, in the velocity variance) as moisture content decreases is compensated in part by a decrease in the correlation scale of log conductivity (and, concurrently, in the correlation scale of the longitudinal component of the velocity). Such an approximation assumes use of Gardner’s (1958) equation to describe unsaturated conductivity as a function of matric potential, and holds as long as the correlation scale of  $\beta$  in Gardner’s equation is relatively small compared with that of log saturated conductivity.

#### D2.2.3.4 Macrodispersivity Estimates for Non-Reactive Species

The Gelhar and Axness (1983) equation can be used to estimate asymptotic values of macrodispersivity. However, to account for the effects of unsaturated flow, a modified version is used:

$$A_L(<h>) = \sigma_{LnK}^2 \lambda \quad \text{Equation D-6}$$

where the longitudinal macrodispersivity depends on the mean tension  $<h>$ .

To apply Equation D-6, an estimate of the vertical correlation scale for unsaturated conductivity is needed. As discussed earlier, a correlation length of the order of about 50 cm was used for sediments at the C tank farm. However, compared to the saturated K values, an increase in the variance of log conductivity is expected to be compensated in part by a decrease in the correlation scale of log unsaturated conductivity. A correlation length of 30 cm is assumed for log unsaturated conductivity for all five strata. Table D-8 provides the log unsaturated conductivity variances and the estimated longitudinal ( $A_L$ ) and transverse ( $A_T$ ) macrodispersivities for various strata. The transverse dispersivities are estimated as 1/10 of the longitudinal values (Gelhar et al. 1992). Gelhar (1993) presented results of stochastic analysis of macrodispersion in unsaturated media by Mantoglou and Gelhar (1985), “Large Scale Models of Transient Unsaturated Flow and Contaminant Transport Using Stochastic Methods.” The large-scale macrodispersivity estimates in Table D-8 are of similar magnitude to those reported for Panoche and Maddock soil types in Gelhar (1993).

**Table D-8. Non-Reactive Macrodispersivity Estimates for Soils at the C Tank Farm**

Strata/Material Type	$\sigma_{LnK}^2$	Correlation length, $\lambda$ cm	$A_L$ cm	$A_T$ cm
Backfill (1) and Cold Creek (pre-Missoula gravels)/Ringold Sandy Gravel (5)	4.54	30	~150	15
Sandy H2 (2)	4.60	30	~150	15
Gravelly sand H3 (3)	4.95	30	~100	10
Gravelly sand H1 (4)	3.19	30	~100	10

### D2.2.3.5 Heterogeneous Sorption Enhanced Macrodispersivities

As expected, the net effect of sorption is to retard the velocity of the contaminant. Because sorption for specific contaminants may be a function of soil properties, as the soil properties experience spatial variability, the sorption also varies (Gelhar 1993; Talbott and Gelhar 1994, *Performance Assessment of a Hypothetical Low-Level Waste Facility: Groundwater Flow and Transport Simulation*). The variation directly affects the velocity of the contaminant, which, in turn, enhances the spreading of the plume. The enhanced spreading is defined by a larger reactive longitudinal macrodispersivity, different from the non-reactive longitudinal macrodispersivity, as discussed in the preceding section. The increased plume spreading due to heterogeneous sorption (over and above the result for no sorption) is defined as the macrodispersivity enhancement. Stochastic theory and field data on contaminant plumes suggest that the effect of macrodispersivity enhancement only occurs in the longitudinal direction. The transverse macrodispersivity is unaffected by sorption variability (Garabedian et al. 1991, "Large-Scale Natural-Gradient Tracer Test in Sand and Gravel, Cape Cod, Massachusetts: 2, Analysis of Spatial Moments for a Nonreactive Tracer").

The only radionuclide considered for sorption enhancement is uranium; other nuclides have zero  $K_d$ . Ideally, to evaluate sorption enhancement, unsaturated hydraulic conductivity measurements and  $K_d$  for each species are needed on the same soil samples. However, this was not possible for the samples utilized in this work.

Stochastic theory developed by Gelhar (1993) was evaluated to determine the importance of varying longitudinal macrodispersivity by contaminant species on the basis of sorption heterogeneity and correlation with hydraulic conductivity. An enhancement of macrodispersivity can have significant effects on the expected contaminant movement predictions for numerical models.

In order to understand the importance of heterogeneous, spatially variable sorption, a number of parameters were defined. The variable  $K_d$  may be prescribed by a mean ( $\bar{K}_d$ ) and a standard deviation ( $\sigma_{K_d}$ ). Further, a retardation factor,  $R$ , was related to  $K_d$  by the following equation:

$$R = 1 + \frac{\rho_b K_d}{\theta} \quad \text{Equation D-7}$$

where  $R$  may be described statistically by an effective retardation,  $\bar{R} = E[R]$ , and its standard deviation,  $\sigma_R$ .

By analyzing the mean and standard deviation of a sample data set of a measured soil property and by showing a relationship between the soil property and  $R$ ,  $\bar{R}$  and  $\sigma_R$  were calculated as a function of the soil property data set.

The net result of the variation in the retardation and the relationship between the retardation and  $\ln K$  is to increase the longitudinal macrodispersivity of the sorbed species according to the following equation given by Talbott and Gelhar (1994):

$$A_{11} = A_0 \left\{ \left[ 1 + \gamma \frac{\sigma_R}{R \sigma_{LnK}} \sqrt{\zeta} \right]^2 + (1 - \zeta) \frac{\sigma_R^2 \lambda_n}{R^2 \sigma_{LnK}^2 \lambda_1} \gamma^2 \right\} \quad \text{Equation D-8}$$

where:

$A_0$  = non-reactive longitudinal macrodispersivity

$\lambda_1$  = horizontal correlation scale,  $\lambda_n \approx \lambda_1$

$\gamma$  = ratio of harmonic to geometric mean for unsaturated  $K$ .

Equation D-8 is identical to that in Talbott and Gelhar (1994), except that the appropriate variables are evaluated for unsaturated conditions. Equation D-8 assumes random  $K_d$  but constant bulk density and moisture content. However, using the more general case (Gelhar 1993, p. 256) when all three (i.e.,  $K_d$ , bulk density, and moisture content) vary, it was found that the contribution to Equation D-8 from variations of bulk density and moisture content were negligibly small, compared to variations of  $K_d$ .

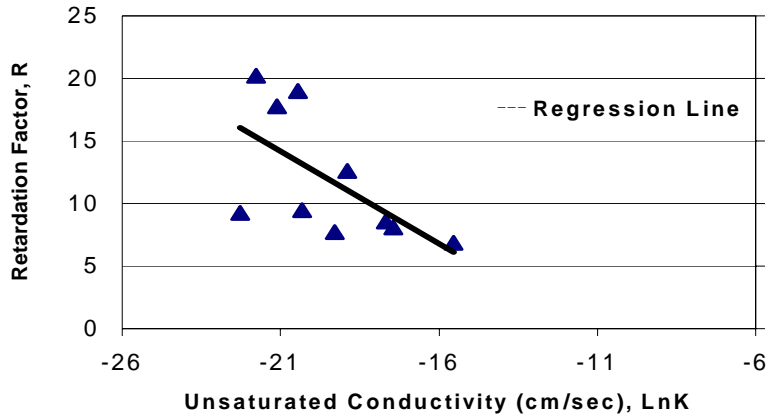
The  $\ln K$  versus  $R$  relation for uranium for various strata are shown in Figure D-8. Results of stochastic analysis for macrodispersivity enhancement for different strata are shown in Table D-9. Note that the unsaturated  $K$  values were evaluated at -100 cm via the fitted van Genuchten-Mualem relation. The macrodispersivity enhancement,  $A_{11}/A_0$ , ranges from about 1.06 for the H2 sandy sediments to about 1.12 for the H1 gravelly sand sediments.

**Table D-9. Macrodispersivity Enhancement Estimates for Various Strata at the C Tank Farm [ $\rho_b$  in  $\text{g}/\text{cm}^3$  and  $K_d$  in  $\text{cm}^3/\text{g}$ ]**

Strata/Material Type	$\bar{K}_d$	$\sigma_{K_d}/\bar{K}_d$	$\bar{R}$	$\sigma_R/\bar{R}$	$\bar{\rho}_b$	$\bar{\theta}$	$\sigma_{LnK}^2$	$\gamma$	$\zeta$	$\lambda_n/\lambda_1$	$A_{11}/A_0$
Backfill (1)/ Cold Creek (pre-Missoula gravels)/ Ringold Sandy Gravel (5)	0.6	0	11.94	0.43	2.13	0.066	4.54	0.26	0.38	1	1.067
Sandy H2 (2)	0.6	0	14.31	0.67	1.76	0.115	4.60	0.13	0.58	1	1.063
Gravelly sand H3 (3)	0.6	0	14.34	0.50	1.94	0.086	4.95	0.20	0.42	1	1.062
Gravelly sand H1 (4)	0.6	0	11.36	0.38	2.07	0.081	3.19	0.32	0.72	1	1.120

**Figure D-8. Uranium LnK versus R for (a) Backfill (1) and Cold Creek (pre-Missoula gravels)/Ringold Sandy Gravel (5), (b) Sandy H2 (2), (c) Gravelly Sand H3 (3), and (d) Gravelly Sand H1 (4) at the C Tank Farm (2 pages)**

(a)



(b)

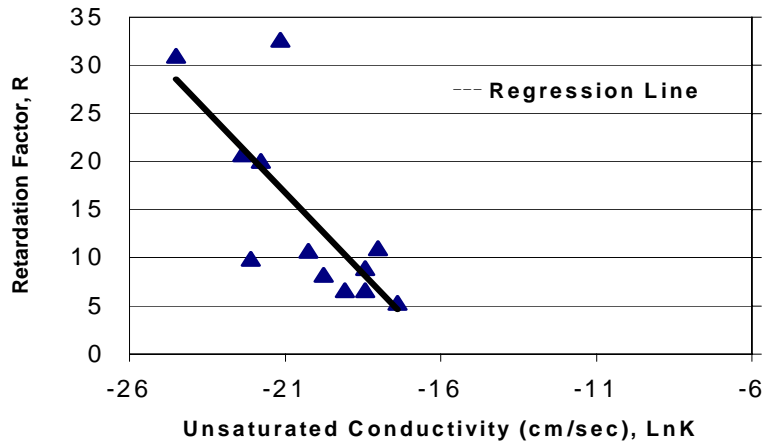
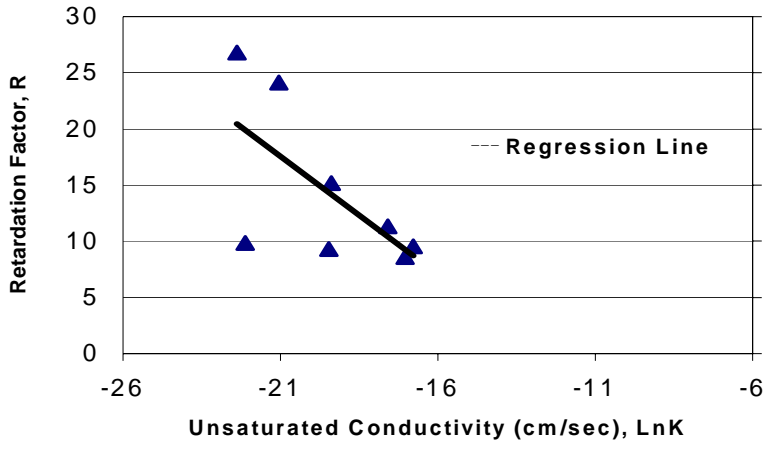
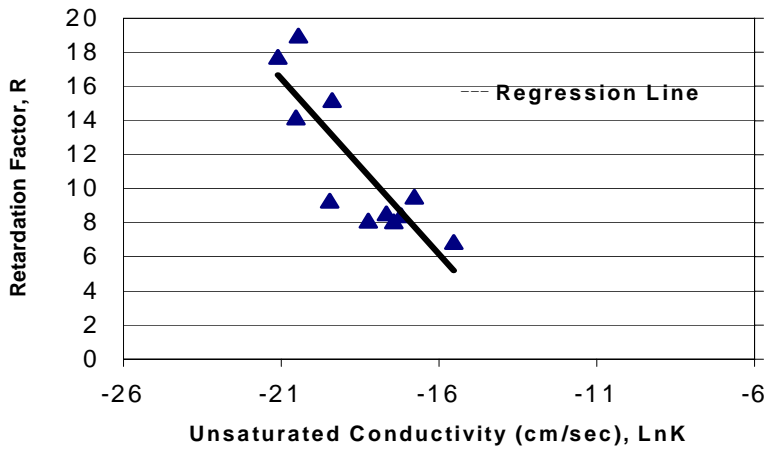


**Figure D-8. Uranium LnK versus R for (a) Backfill (1) and Cold Creek (pre-Missoula gravels)/Ringold Sandy Gravel (5), (b) Sandy H2 (2), (c) Gravelly Sand H3 (3), and (d) Gravelly Sand H1 (4) at the C Tank Farm (2 pages)**

(c)



(d)



**D3.0 REFERENCES**

- Bear, J., C. Braester, and P.C. Menier, 1987, "Effective and Relative Permeabilities of Anisotropic Porous Media," *Transport in Porous Media*, Vol. 2, pp. 301-316.
- Dagan, G., 1984, "Solute Transport in Heterogeneous Porous Formations," *J. Fluid Mech.*, Vol. 145, pp. 151-157.
- Freeze, R.A., and J.A. Cherry, 1979, *Groundwater*, Prentice-Hall, Inc., Englewood Cliffs, New Jersey.
- Garabedian, S.P., D.R. LeBlanc, L.W. Gelhar, and M.A. Celia, 1991, "Large-Scale Natural Gradient Tracer Test in Sand and Gravel, Cape Cod, Massachusetts: 2, Analysis of Spatial Moments for a Nonreactive Tracer," *Water Resources Research*, Vol. 27(5), pp. 911-924.
- Gardner, W.H., 1986, "Water Content," *Methods of Soils Analysis*, Part I, edited by A. Klute, pp. 493-544, American Society of Agron, Madison, Wisconsin.
- Gardner, W.R., 1958, "Some Steady-State Solutions of the Unsaturated Moisture Flow Equation with Applications to Evaporation from a Water Table," *Soil Science*, Vol. 85, pp. 228-232.
- Gelhar, L.W., C. Welty and K.R. Rehfeldt, 1992, "A Critical Review of Data on Field-Scale Dispersion in Aquifers," *Water Resources Research*, Vol. 28, pp. 1955-1974.
- Gelhar, L.W., 1993, *Stochastic Subsurface Hydrology*, Prentice Hall, New York.
- Gelhar, L.W., and C.L. Axness, 1983, "Three-Dimensional Analysis of Macrodispersion in a Stratified Aquifer," *Water Resources Research*, Vol. 19, pp. 161-180.
- Green, T.R., and D.L. Freyberg, 1995, "State-Dependent Anisotropy: Comparisons of Quasi-Analytical Solutions with Stochastic Results for Steady Gravity Drainage," *Water Resources Research*, Vol. 31(9), pp. 2201-2212.
- Hills, R.G., P.J. Wierenga, D.B. Hudson, and M.R. Kirkland, 1991, "The Second Las Cruces Trench Experiment: Experimental Results and Two-Dimensional Flow Predictions," *Water Resources Research*, Vol. 27(10), pp. 2707-2718.
- Kaplan, D.L., and R.J. Serne, 2000, *Geochemical Data Package For the Immobilized Low-Activity Waste Performance Assessment (ILAW PA)*, PNNL-13037, Rev. 1, Pacific Northwest National Laboratory, Richland, Washington.
- Khaleel, R., and J.F. Relyea, 1997, "Correcting Laboratory-Measured Moisture Retention Data for Gravels," *Water Resources Research*, Vol. 33, pp. 1875-1878.
- Khaleel, R., J.F. Relyea, and J.L. Conca, 1995, "Evaluation of van Genuchten-Mualem Relationships to Estimate Unsaturated Conductivity at Low Water Contents," *Water Resources Research*, Vol. 31, pp. 2659-2668.

- Khaleel, R., and E.J. Freeman, 1995, *Variability and Scaling of Hydraulic Properties for 200 Area Soils, Hanford Site*, WHC-EP-0883, Westinghouse Hanford Company, Richland, Washington.
- Kincaid, C.T., J.W. Shade, G.A. Whyatt, M.G. Piepho, K. Rhoads, J.A. Voogd, J.H. Westsik, Jr., M.D. Freshley, K.A. Blanchard, B.G. Lauzon, 1995, *Performance Assessment of Grouted Double-Shell Tank Waste Disposal at Hanford*, WHC-SD-WM-EE-004, Rev. 1, Westinghouse Hanford Company, Richland, Washington.
- Klute, A., 1986, "Water Retention: Laboratory Methods," *Methods of Soils Analysis*, Part I, edited by A. Klute, pp. 635-660, American Society of Agron, Madison, Wisconsin.
- Klute, A., and C. Dirksen, 1986, "Hydraulic Conductivity and Diffusivity: Laboratory Methods," *Methods of Soils Analysis*, Part I, edited by A. Klute, pp. 687-734, American Society of Agron, Madison, Wisconsin.
- Mantoglou, A., and L.W. Gelhar, 1987, "Stochastic Modeling of Large-Scale Transient Unsaturated Flow," *Water Resources Research*, Vol. 23, pp. 37-46.
- Mantoglou, A., and L.W. Gelhar, 1985, "Large Scale Models of Transient Unsaturated Flow and Contaminant Transport Using Stochastic Methods," Ralph M. Parsons Laboratory Technical Report 299, Massachusetts Institute of Technology, Cambridge, Massachusetts.
- McCord, J.T., D.B. Stephens, and J.L. Wilson, 1991, "Hysteresis and State-Dependent Anisotropy in Modeling Unsaturated Hillslope Hydrologic Processes," *Water Resources Research*, Vol. 27(7), pp. 1501-1518.
- Millington, R.J., and J.P. Quirk, 1961, "Permeability of Porous Solids," *Trans. Faraday Soc.*, Vol. 57, pp. 1200-1207.
- Mualem, Y., 1984, "Anisotropy of unsaturated soils," *Soil Sci. Soc. Am. J.*, Vol. 48, pp. 505-509.
- Mualem, Y., 1976, "A New Model for Predicting the Hydraulic Conductivity of Unsaturated Porous Media," *Water Resources Research*, Vol. 12, pp. 513-522.
- Phillips, F.M., J.L. Mattick, T.A. Duval, D. Elmore, and P.W. Kubik, 1988, "Chlorine-36 and Tritium from Nuclear-Weapons Fallout as Tracers for Long-Term Liquid and Vapor Movement in Desert Soils," *Water Resources Research*, Vol. 24(11), pp. 1877-1891.
- Polmann, D.J., 1990, *Application of Stochastic Methods to Transient Flow and Transport in Heterogeneous Unsaturated Soils*, Ph.D. Thesis, Massachusetts Institute of Technology, Cambridge, Massachusetts.
- Russo, D., 1993, "Stochastic Modeling of Macrodispersion for Solute Transport in a Heterogeneous Unsaturated Porous Formation," *Water Resources Research*, Vol. 29, pp. 383-397.

- Scanlon, B.R., 1992, "Evaluation of Liquid and Vapor Water Flow in Desert Soils Based on Chlorine 36 and Tritium Tracers and Nonisothermal Flow Simulations," *Water Resources Research*, Vol. 28(1), pp. 285-297.
- Sisson, J.B., and A.H. Lu, 1984, *Field Calibration of Computer Models for Application to Buried Liquid Discharges: A Status Report*, RHO-ST-46P, Rockwell Hanford Operations, Richland, Washington.
- Stephens, D.B., and S. Heermann, 1988, "Dependence of Anisotropy on Saturation in a Stratified Sand," *Water Resources Research*, Vol. 24(5), pp. 770-778.
- Talbott, M.E., and L.W. Gelhar, 1994, *Performance Assessment of a Hypothetical Low-Level Waste Facility: Groundwater Flow and Transport Simulation*, NUREG/CR-6114, Vol. 3, U.S. Nuclear Regulatory Commission, Washington, D.C.
- van Genuchten, M.Th., 1980, "A Closed-Form Solution for Predicting the Conductivity of Unsaturated Soils," *Soil Sci. Soc. Am. J.*, Vol. 44, pp. 892-898.
- van Genuchten, M.Th., F.J. Leij, and S.R. Yates, 1991, *The RETC Code for Quantifying the Hydraulic Functions of Unsaturated Soils*, U.S. E.P.A., EPA/600/2-91/065.
- Ward, A.L., R.E. Clayton, and J.S. Ritter, 1998, *Determination of In Situ Hydraulic Parameters of the Upper Hanford Formation*, Letter Report to Fluor Daniel Northwest, Inc., from Pacific Northwest National Laboratory, Richland, Washington.
- WHC, 1991, *Geotechnical Engineering Procedure Manual*, Vols. 1 and 2, WHC-EP-0635, Westinghouse Hanford Company, Richland, Washington.
- Wierenga, P.J., R.G. Hills, and D.B. Hudson, 1991, "The Las Cruces Trench Site: Characterization, Experimental Results, and One-Dimensional Flow Predictions," *Water Resources Research*, Vol. 27(10), pp. 2695-2705.
- Yeh, T.-C.J., and D.J. Harvey, 1990, "Effective Unsaturated Hydraulic Conductivity of Layered Sands," *Water Resources Research*, Vol. 26(6), pp. 1271-1279.
- Yeh, T.-C.J., L.W. Gelhar, and A.L. Gutjahr, 1985a, "Stochastic Analysis of Unsaturated Flow in Heterogeneous Soils, 1, Statistically Isotropic Media," *Water Resources Research*, Vol. 21, pp. 447-456.
- Yeh, T.-C.J., L.W. Gelhar, and A.L. Gutjahr, 1985b, "Stochastic Analysis of Unsaturated Flow in Heterogeneous Soils, 2, Statistically Anisotropic Media with Variable  $\alpha$ ," *Water Resources Research*, Vol. 21, pp. 457-464.
- Yeh, T.-C.J., L.W. Gelhar, and A.L. Gutjahr, 1985c, "Stochastic Analysis of Unsaturated Flow in Heterogeneous Media, 3, Observations and Applications," *Water Resources Research*, Vol. 21, pp. 465-471.